HEAVY-FERMION PHENOMENA

D. W. HESS, *Naval Research Laboratory, Washington, D.C., U.S.A.*
P. S. RISEBOROUGH, *Polytechnic University, Brooklyn, New York, U.S.A.*
J. L. SMITH, *Los Alamos National Laboratory, Los Alamos, New Mexico, U.S.A.*

INTRODUCTION

Solid-state compounds containing rare-earth or actinide elements can display a wide variety of unusual behavior, including magnetic order, mixed valence, and heavy-fermion phenomena. These various behaviors reflect the quantum state of the electrons derived from atomic f orbitals. The heavy-fermion systems have almost localized electronic states at the Fermi surface that are primarily f in character. The electrons in these states interact strongly and give rise to an unusual transformation evident at low temperature. Near room temperature ($\sim$300 K), the sublattice of rare-earth or actinide atoms, usually cerium or uranium, has properties resembling those of weakly interacting magnetic moments immersed in a sea of conduction electrons. The electronic transport properties are dominated by incoherent scattering of the conduction electrons by the local moments. As the temperature is lowered, local-moment behavior gives way to electronic properties that are consistent with those of a narrow band of conduction electrons. A crossover temperature, often referred to as the "coherence temperature" T^*, can be inferred from experiments. At sufficiently low temperature, the thermodynamic properties of a system of itinerant electrons may be described in terms of thermal effective masses for the electrons. The electronic effective masses in most metals do not differ much from the mass of a free electron. In contrast, the effective mass deduced from experiments on the heavy-fermion systems is up to 1000 times greater than that of a free electron. Hence these materials were christened with the somewhat whimsical name "heavy-fermion systems."

Heavy-fermion systems display a variety of ground states including antiferromagnetic, superconducting, paramagnetic (at least to the lowest temperatures at which experiments have been performed, $\sim$20 mK), or, as recently observed, semiconducting. Table 1 lists some of the heavy-fermion systems with their ground states and ordering temperatures where appropriate. Note that superconductivity and antiferromagnetism often coexist, with the Néel temperature T_N typically being about an order of magnitude larger than the critical temperature T_c of the superconducting state.

1-56081-066-1/93/$5.00+.50

Table 1. Some heavy-electron systems.[a]

Principal order	Compound	Ordering Temperature (K) T_c	T_N
Superconductors	$CeCu_2Si_2$	0.65	
	UBe_{13}	0.90	
	UPt_3	0.5	5.0
	URu_2Si_2	1.5	17.0
	UPd_2Al_3	2.0	14.0
Antiferromagnets	U_2Zn_{17}	—	9.7
	UCd_{11}	—	5.0
	UCu_5	—	15.2
	$CePt_2Sn_2$	—	0.88
No long-range ordering to 0.02 K	$CeAl_3$	—	—
	$CeCu_6$	—	—
	$YbAgCu_4$	—	—
	UAl_2	—	—
		Gap (K)	
Semiconductors	CeNiSn	6.0	
	$Ce_3Bi_4Pt_3$	35.0	

[a]Data from Fisk *et al.* (1988); $CePt_2Sn_2$, Beyermann *et al.* (1991); $YbAgCu_4$, Rossel *et al.* (1987); CeNiSn, Takabatake *et al.* (1990); $Ce_3Bi_4Pt_3$, Hundley *et al.* (1990); and UPd_2Al_3, Amato *et al.* (1992).

Heavy-fermion systems generally appear to be close to an instability, as suggested by the proclivity of many of these systems to display an ordered ground state on the addition of impurities, on the application of a magnetic field, and possibly on the application of pressure.

The low-temperature properties of some heavy-fermion materials display similarities to those of the archetypal Fermi liquid, liquid ^{3}He. In particular, the specific heat of liquid ^{3}He varies linearly with temperature, and the magnetic susceptibility is temperature independent. Both of these quantities are considerably larger than expected for a weakly interacting collection of ^{3}He atoms because of large many-body effects. The low-temperature properties of ^{3}He are well described by the phenomenological Landau Fermi-liquid theory. In the heavy-fermion systems, the specific heat and magnetic susceptibility are also greatly enhanced by many-body effects, and it is generally accepted that the low-temperature properties of these materials can also be described by Landau Fermi-liquid theory. It was hoped that analogies with liquid ^{3}He would help clarify the role of the many-body problem in understanding the physics of the "coherent" heavy-fermion state even though they suffer greatly from oversimplification. Liquid ^{3}He is after all isotropic and translationally invariant, and has only two spin states in contradistinction to the potentially manyfold-degenerate f electrons constrained to the symmetry of a crystalline lattice.

In seeking to describe not only the Fermi-liquid state, but also the process whereby a lattice of f moments immersed in a sea of conduction electrons becomes a Fermi liquid, microscopic approaches exploit the apparent similarity to the Kondo model. The Kondo model consists of a single impurity atom with a magnetic moment embedded in a metallic host. The heavy-fermion materials may be viewed as a lattice of f atoms, each with a magnetic moment, embedded in a metallic matrix; a compelling example is UBe_{13}. At high temperatures the lattice reflects the properties of independent magnetic impurities, and as the temperature is reduced one expects to observe the many-body effects characteristic of the single impurity model. At even lower temperatures, the interactions between impurities become important and the magnetic scattering from the lattice becomes coherent, leading to the formation of Bloch states with narrow bandwidths. A generalization of a system of dense, periodically arranged, single impurities, such as the Anderson lattice model

described below, is believed to contain the essential physics of the heavy-fermion phenomenon.

Quite apart from the issue of the formation of the heavy-fermion state itself is the nature of the ordered states. In every case, the ground state listed in Table 1 is unusual as compared to the corresponding ground state encountered in most other materials. The magnetic state is characterized by anomalously small moments associated with the *f*-atom sites. The arrangement of these moments is simple in contrast with the spiral phases often observed in rare-earth magnets. The most studied ordered state is the unusual superconducting state, which is not described by the BCS theory for a conventional superconductor. The analogies between heavy-fermion systems and ^{3}He extend beyond the normal state. Below ~1 mK, the normal state of ^{3}He becomes unstable to the formation of a superfluid state in which the pairing of atoms gives rise to a condensate. A comparison of the properties of the heavy-fermion superconducting state to those of superfluid ^{3}He suggests the possibility of unconventional superconductivity in heavy-fermion systems. The conventional superconducting state is described by an order parameter that is a complex scalar function having the symmetry of the point group of the underlying crystalline lattice. In an unconventional superconductor, as in the unconventional superfluid ^{3}He, one or more of these symmetries may be broken (Rainer, 1988). The order parameter may have more degrees of freedom than its conventional counterpart, and different superconducting phases may be degenerate. The possible consequences of such an order parameter include the existence of domain walls separating different superconducting phases and exotic vortices with complicated core structures; neither of these occurs in a conventional superconductor. The superfluid state of ^{3}He is also unusual because spin fluctuations are believed to provide the attractive effective interaction that results in the pairing of ^{3}He atoms. In an ordinary superconductor where the electron-phonon interaction provides the effective attractive interaction between electrons, spin-fluctuation-mediated interactions are unfavorable to the pairing. The analogy with liquid ^{3}He further suggests that the attractive effective interaction between electrons in the heavy-fermion systems is not provided by the electron-phonon interaction as in ordinary superconductors, but rather is electronic in origin and mediated by spin fluctuations.

While much progress has been made over the past decade, a comprehensive understanding of the heavy-fermion phenomenon is still lacking. It should not be surprising, then, that some of the material presented below, particularly the simple interpretations of various experiments, appears in some cases to be contradictory; this is the nature of the field. Below, we attempt to provide a necessarily incomplete overview of the properties of these materials and of the physical picture that has evolved. One of the most exciting aspects of the heavy-fermion phenomenon is the possibility that they may be unconventional superconductors, which serves as the primary focus of our discussion of the superconducting state. Because of the nature of this article, it is not possible to discuss the many key investigations that have led to the current picture of this phenomenon. It is also not always possible to refer to the original scientific literature, and we direct the reader to the more extensive reviews listed in the Works Cited and under Further Reading.

1. EXPERIMENTS

1.1 Background

Heavy-fermion materials occur in a variety of crystal structures as shown by the examples in Table 2. Many of the heavy-fermion systems have crystal structures of uniaxial symmetry and, as expected, exhibit anisotropic properties. The degree of the anisotropy may be unusually large, as we will see below. A common feature of the crystal structures of heavy-fermion systems is that they all have a center of inversion symmetry, a fact that has important consequences for the classification of possible superconducting states. Ott and Fisk (1987) observe another common feature of the crystal structures of heavy-fermion systems: the nearest neighbors of an *f* atom do not include another *f* atom. The large separation between *f* atoms suggests that the transfer matrix elements directly connecting *f* orbitals on different sites are small.

In spite of the large separation between *f*

atoms, these materials are not typical local-moment magnets. Specific-heat experiments played an important role in the discovery of the heavy-fermion phenomenon. While it was known in the 1970s that the properties of $CeAl_3$ below 0.1 K were consistent with those expected for a Fermi liquid characterized by quasiparticles with an anomalously large effective mass (Andres *et al.*, 1975), it was unclear whether this was the correct interpretation of the data. Steglich *et al.* (1979), showed that $CeCu_2Si_2$, a compound with low-temperature properties similar to those of $CeAl_3$, is a superconductor with a specific-heat jump at the transition temperature consistent with superconducting electrons with large effective masses. This was not conclusive at the time because $CeCu_2Si_2$ is difficult to prepare and may contain impurity phases. The large specific-heat jump could be the result of antiferromagnetic ordering (such as in $NpSn_3$), which has a temperature-dependent specific heat similar to that of a BCS superconductor. The "apparent" superconductivity could then be explained by the existence of some impurity phase. The discovery of superconductivity with a similarly large specific-heat jump in UBe_{13} by Ott *et al.* (1983) confirmed the interpretation based on large effective masses, because UBe_{13} lacks the materials problems associated with $CeCu_2Si_2$ but shows similar low-temperature behavior. Other heavy-fermion materials were soon discovered.

Table 2. Crystal structures of some heavy-fermion systems.

Compound	Symmetry	Full-symmetry group
$CeCu_2Si_2$	Tetragonal	$I4/mmm$
UBe_{13}	Cubic	$Fm\bar{3}c$
UPt_3	Hexagonal	$P6_3/mmc$
URu_2Si_2	Tetragonal	$I4/mmm$
UPd_2Al_3	Hexagonal	$P6/mmm$
U_2Zn_{17}	Rhombohedral	$P\bar{6}m2$
UCd_{11}	Cubic	$Pm\bar{3}m$
UCu_5	Cubic	$F\bar{4}3m$
$CeAl_3$	Hexagonal	$P6_3/mmc$
$CeCu_6$	Orthorhombic	$Pnma$
$YbAgCu_4$	Cubic	$F\bar{4}3m$
UAl_2	Cubic	$Fd\bar{3}m$
CeNiSn	Tetragonal	$I4_1md$
$Ce_3Bi_4Pt_3$	Cubic	$I\bar{4}3d$
$CePt_2Sn_2$	Tetragonal	$P4/nmm$

1.2 Normal-State Properties

1.2.1 Specific Heat. The low-temperature specific heat of the metallic heavy-fermion systems differs dramatically from that of an ordinary metal. For temperatures much smaller than the Fermi energy and the Debye temperature, the specific heat of an ordinary metal consists of an electronic contribution linear in temperature and a contribution from phonons,

$$C(T)=\gamma T+\beta T^3. \qquad (1)$$

The specific heat of an ordinary metal may be understood by comparing γ with that expected for a gas of electrons neglecting interactions, γ_0. At low temperatures, only excitations in the vicinity of the Fermi surface are important. As a result of the interaction of an electron with the periodic potential of the lattice and with other electrons, these excitations are not those of single electrons but rather quasiparticles, which have an effective mass different from the mass of a free electron. Quasiparticle excitations are probed in a low-temperature specific-heat measurement, and the ratio γ/γ_0 provides a rough measure of the effect of interactions. In a metal such as sodium, the energy bands are broad and free-electron-like; the interaction of an electron with lattice excitations is relatively weak; the effective mass of the quasiparticle does not differ much from the free-electron mass; and γ/γ_0 is ~ 1.3. In contrast, enormous γ/γ_0 ratios up to 1000 are inferred for the metallic heavy-fermion systems.

The specific heat of copper is described well by Eq. (1) for temperatures below 10 K with $\gamma \sim 1$ mJ/mol K^2. In many of the heavy-fermion systems, notably UBe_{13}, $CeCu_2Si_2$, $CeAl_3$, and $CeCu_6$, $\gamma(T)\equiv C(T)/T$ shows a strong upturn with decreasing temperature below ~ 10 K, as shown in Fig. 1 for UBe_{13}. With further reduction in temperature $\gamma(T)$ may show a weak maximum, but eventually it tends to a value ~ 1 J/(mol *f*-atom K^2). Table 3 shows extrapolated values of $\gamma(0)=\lim_{T\to 0}C_p(T)/T$ for some heavy-fermion systems. The specific heat of UPt_3 and UAl_2 has been fitted by the expression

$$C(T)=\gamma T+\delta T^3\ln T+\beta T^3 \qquad (2)$$

for temperatures up to 20 K. This form is suggestive of a strongly interacting Fermi liquid and will be discussed further below.

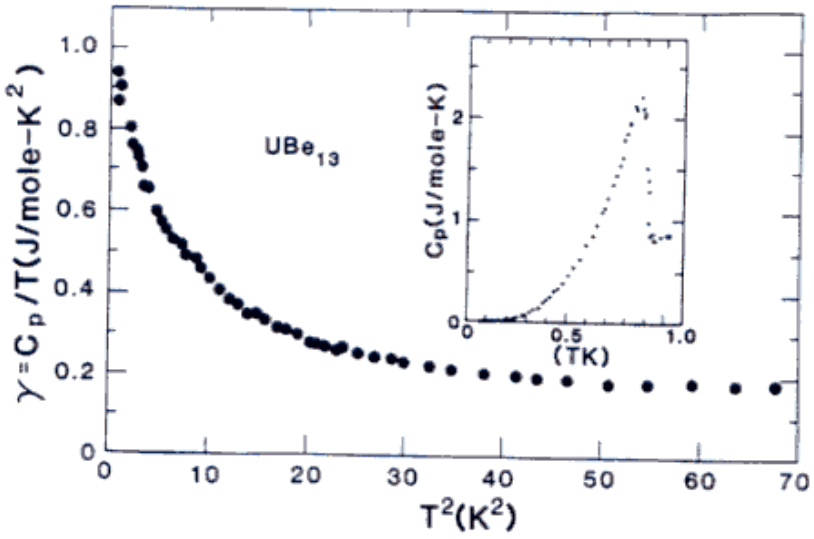

FIG. 1. The specific heat of UBe_{13} divided by temperature, $\gamma(T)$ (Ott *et al.*, 1983), in the normal state. Note the upturn with decreasing temperature and the large extrapolated value of $\gamma(0)$ as compared with 0.07 mJ/mole-K^2 for copper. The inset shows the specific-heat jump at the superconducting transition, indicating that the enormous $\gamma(0)$ should be associated with itinerant electrons.

The antiferromagnets U_2Zn_{17} and UCd_{11} are unusual in that $\gamma(T)$ has already reached a saturation value by 10 K. As discussed in detail by Ott and Fisk (1987), UCu_5 is also unusual in that the characteristic heavy-fermion upturn in $\gamma(T)$ appears below the antiferromagnetic phase transition at 15 K. Thus although a gap associated with magnetic order appears over a major fraction of the Fermi surface, the mechanism that gives rise to the formation of the heavy-fermion state is still operative.

Specific-heat experiments at low temperature also show that the heavy-fermion state is sensitive to impurities and to the application of pressure. For example, substitution of thorium for 3.3% of the uranium atoms in UBe_{13} causes the upturn of $\gamma(T)$ to appear at

Table 3. Low-temperature properties of some heavy-electron systems. Properties for anisotropic systems are given along the principal directions in the form "*a*/*b*/*c*" when data on single crystals are available.[a]

Compound	$\gamma(0)$ (mJ/mol *f*-atom K^2)	$\chi(0)$ (10^{-3} emu cm^{-3})	ρ_0 ($\mu\Omega$ cm)	ρ_{ee} ($\mu\Omega$ cm K^{-2})
$CeCu_2Si_2$	1000	0.13	4.8	10.7
UBe_{13}	1100	0.18	18	—
UPt_3	450	0.19/0.19/0.10	0.5	0.5
URu_2Si_2	180	0.03/0.03/0.10	33	0.17/0.17/0.10
UPd_2Al_3	150	0.14	3.5	—
U_2Zn_{17}	500	0.19/0.19/0.24	—	—
UCd_{11}	840	0.24	—	—
UCu_5	>250	0.18	—	—
$CeAl_3$	1620	0.41	0.77	35
$CeCu_6$	1300	0.28	18.1/5.71/10.6	—
UAl_2	142	0.13	4.8	10.7
$CePt_2Sn_2$	10 000	0.30	57	—
$YbAgCu_4$	245	0.47	14	0.06

[a]Data from Fisk *et al.* (1988); $CePt_2Sn_2$, Beyermann *et al.* (1991); $YbAgCu_4$, Rossel *et al.* (1987); CeNiSn, Takabatake *et al.* (1990); $Ce_3Bi_4Pt_3$, Hundley *et al.* (1990); UPd_2Al_3, Amato *et al.* (1992).

lower temperatures and leads to a substantial increase in $\gamma(0)$. A similar replacement of uranium by lutetium causes the opposite effect, resulting in a ~25% decrease in $\gamma(0)$. In $CeAl_3$, UBe_{13}, $CeCu_6$, and $CeCu_2Si_2$ the application of 1 GPa pressure leads to a 30% to 50% decrease in $\gamma(0)$. Evidently some impurity substitutions lead to a contraction of the lattice and have essentially the same effect as the application of pressure.

1.2.2 Magnetic Susceptibility. An interesting crossover between local-moment and narrow-band regimes can be seen in the magnetic susceptibility as a function of temperature for the heavy-fermion systems as shown in Fig. 2 for UBe_{13} and $CeAl_3$. Near room temperature, the susceptibility $\chi(T)$ displays a Curie-Weiss temperature dependence,

$$\chi_{CW}(T)=\frac{n}{3k_B}\frac{\mu_{eff}^2}{(T-\Theta_{CW})}, \tag{3}$$

where μ_{eff} is the size of the local moment, Θ_{CW} is the Curie-Weiss temperature, n is the density of local moments, and k_B is Boltzmann's constant. The values of μ_{eff} and Θ_{CW} obtained from fitting $\chi(T)$ by Eq. (3) appear in Table 4 for some heavy-fermion systems. The effective moments deduced from the data are roughly the same as those expected from Hund's rules for free f atoms with integral f occupancy, which are also shown in Table 4 for comparison. The values of Θ_{CW} are always negative and lie between 8 K and room temperature. A detailed discussion of the sensitivity of these fits to the temperature range over which they are performed appears in Ott and Fisk (1987).

At low temperature, $\chi(T)$ is weakly temperature dependent and resembles a Pauli susceptibility. For a gas of noninteracting electrons, the Pauli susceptibility and linear specific-heat coefficient are related to the density of states at the Fermi energy $N(e_F)$ through

$$\chi_P=\mu_B^2 N(e_F), \tag{4}$$

$$\gamma=\frac{\pi^2}{3}k_B^2 N(e_F), \tag{5}$$

and so a plot of γ vs χ_P for various free-electron-like systems lies along the line $\gamma=(\pi^2/3)(k_B/\mu_B)^2\chi_P$. The heavy-fermion systems, especially the superconductors, lie quite near this line (Fisk *et al.*, 1985), indicating that the low-temperature magnetic susceptibility and specific heat are enhanced by roughly the same amount. The crossover between these distinct temperature dependences occurs abruptly relative to the upturn in the specific heat, suggesting the existence of a characteristic energy scale.

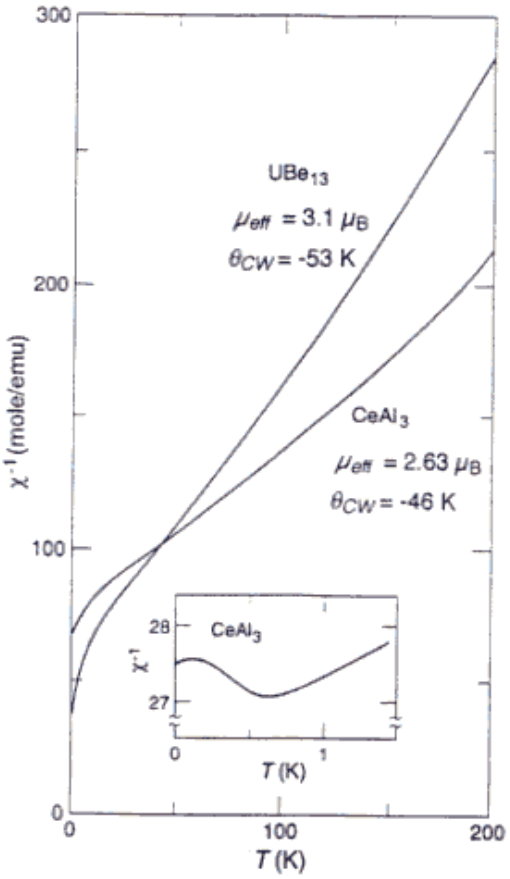

FIG. 2. The magnetic susceptibility $\chi(T)$ of UBe_{13} and $CeAl_3$ plotted as $\chi^{-1}(T)$. The effective moments and Curie-Weiss temperature from a fit by a Curie-Weiss form at high temperatures are also shown. The temperature dependence of $\chi(T)$ weakens with decreasing temperature and becomes Pauli type as shown for $CeAl_3$ in the inset. This is not apparent in UBe_{13}, as a transition to the superconducting state occurs before any behavior consistent with Landau Fermi-liquid theory is observed.

The magnetic susceptibilities of many of the heavy-fermion compounds are anisotropic. A particularly striking example is that of URu_2Si_2, for which $\chi(T)$ for fields in the basal plane is nearly temperature independent up to room temperature whereas $\chi(T)$ for fields applied along the c axis displays the classic heavy-fermion behavior outlined above. In

Table 4. High-temperature properties of some heavy-electron systems. Properties for anisotropic systems are given along the principal directions in the form "a/b/c" when data on single crystals are available.[a]

Compound	$-\Theta_{CW}$ (K)	μ_{eff} (μ_B)	$\rho(T=300K)$ ($\mu\Omega$ cm)
$CeCu_2Si_2$	140	2.68	90
UBe_{13}	53	3.1	107
UPt_3	50/170	2.6/2.6	130
URu_2Si_2	—/—/65	—/—/3.51	324/324/169
UPd_3Al_3	47	3.2	140
U_2Zn_{17}	105	3.3	110
UCd_{11}	23	3.45	80
UCu_5	284	3.52	286
$CeAl_3$	46	2.63	65
$CeCu_6$	59/59/18	2.6/2.67/2.46	70/70/70
UAl_2	245	3.1	190
CeNiSn	—	—	206/187/125
$Ce_3Bi_4Pt_3$	125	~2.45	250
$CePt_2Sn_2$	25	2.59	~140
$YbAgCu_4$	31	4.28	~100

f configuration	Hund's-rule moment
f^1	2.54
f^2	3.58
f^3	3.62

[a]Data from Fisk *et al.* (1988); $CePt_2Sn_2$, Beyermann *et al.* (1991); $YbAgCu_4$, Rossel *et al.* (1987); CeNiSn, Takabatake *et al.* (1990); $Ce_3Bi_4Pt_3$, Hundley *et al.* (1990); UPd_2Al_3, Amato *et al.* (1992); UPt_3; de Visser (1986).

the limit of zero temperature, $\chi_c(0)/\chi_a(0) \sim 5$. A less dramatic but still large anisotropy exists for UPt_3. There the basal-plane susceptibility is nearly three times that along the c axis and shows a peak at 17 K.

1.2.3 Thermal Expansion. The thermal expansion coefficient of the heavy-fermion systems below room temperature is positive and strongly temperature dependent. A peak in the thermal expansion as a function of temperature is evident for some materials, while others show a thermal expansion that decreases monotonically with temperature. At low temperatures, the thermal expansion is anomalously large by two or more orders of magnitude.

The thermal expansion is often expressed as a Grüneisen parameter,

$$\Gamma = \frac{\alpha_v V_m}{\kappa C}, \tag{6}$$

where $\alpha_v = (1/V)\partial V/\partial T$ is the coefficient of volume thermal expansion, κ is the (isothermal) compressibility, V_m is the molar volume, and C is the molar specific heat. In an ordinary metal, the low-temperature thermal expansion tracks the specific heat, and Γ is essentially temperature independent. The Grüneisen parameter for a heavy-fermion system increases strongly with decreasing temperature below 10 K. In analogy with the contribution to Γ from the lattice, which is often described by the volume derivative of the Debye temperature, the temperature dependence of Γ is interpreted as the result of a single electronic energy scale, T^*, and an electronic Grüneisen parameter is defined, $\Gamma_e = -\partial \ln T^*/\partial \ln V$. The elastic constants, magnetostriction, and thermal expansion are interrelated by this model as discussed in some detail by Fulde *et al.* (1988).

1.2.4 de Haas–van Alphen Effect. Detailed information on the geometry of the Fermi surface and the cyclotron effective masses can be obtained from the observation of oscillations in the magnetization as a function of the reciprocal magnetic induction. In ascertaining the shape of the Fermi surface, electronic band-structure calculations have traditionally been used as a guide, and for

most ordinary metals, calculations and experiment are in good agreement. Generally speaking, the Fermi surface can have many sheets resulting from different bands crossing the Fermi energy. Consider a single sheet. In Fermi-liquid theories, the fundamental frequency of the oscillations gives the area of the extremal cross section of the Fermi surface perpendicular to the applied field. The temperature dependence of the amplitude is related to the cyclotron effective mass, which in turn is related to an average of the Fermi velocity over the perimeter of the extremal cross section. Although the cyclotron effective mass is not rigorously equal to the thermal effective mass, using the Fermi velocities deduced from a de Haas–van Alphen experiment to estimate the specific heat usually gives a result near the measured value.

To observe these oscillations, the mean free path l of a quasiparticle must be larger than a quasiparticle cyclotron radius,

$$l \gg v_F/\omega_H , \tag{7}$$

and the thermal smearing at the Fermi surface must be sufficiently small,

$$T \ll \omega_H . \tag{8}$$

Here v_F is the Fermi velocity, and $\omega_H = eH/m^*c$ is the effective cyclotron frequency of quasiparticles of charge e and effective mass m^* in a field H. For large effective masses and short mean free paths, these constraints suggest that the experiment should be performed at low temperature and high field. It is important to note that the amplitude of oscillation depends exponentially on the effective mass of the quasiparticles. Lighter quasiparticles produce a larger signal and are thus more easily observed.

Experiments have been performed on UPt_3, $CeRu_2Si_2$, and $CeCu_6$ for temperatures ~20–100 mK and fields up to ~14 T. In all cases unusually large effective masses have been observed. For UPt_3, the Fermi surface geometry is in good agreement with that obtained from electronic structure calculations (Taillefer *et al.*, 1987). The effective mass on any given sheet of the Fermi surface, however, is some 10 to 30 times larger than that obtained from band-structure calculations (Wang *et al.*, 1987) suggesting significant many-body effects. The effective masses range from 25 to 200 times the mass of a free electron. The ratio of the effective masses to those predicted by band theory is roughly the same as the ratio of the measured specific heat to that obtained using electronic structure calculations. UPt_3 shows only heavy masses at the Fermi surface, including the largest effective mass ever measured by the de Haas–van Alphen technique. In contrast, lighter electrons are evident in $CeCu_6$ and $CeRu_2Si_2$. Experiments on $CeCu_6$ (Chapman *et al.*, 1990) find effective masses in the range $(6–80)m_e$ and a Fermi-surface geometry that is neither similar to $LaCu_6$, which has no f electrons, nor to $PrCu_6$, which has f electrons localized in nearly atomic orbitals. Comparisons with specific-heat measurements suggest that unobserved heavier bands exist. Observed electron effective masses for $CeRu_2Si_2$ lie roughly in the range $(1–20)\ m_e$.

1.2.5 Transport Properties. At room temperature, the resistivity of a heavy-fermion compound is large, typically of order 100 $\mu\Omega$/cm as shown in Table 4. In contrast to ordinary metals, where $\partial\rho/\partial T > 0$, $d\rho/dT$ can be of either sign. The qualitative behaviors observed for the resistivity as a function of

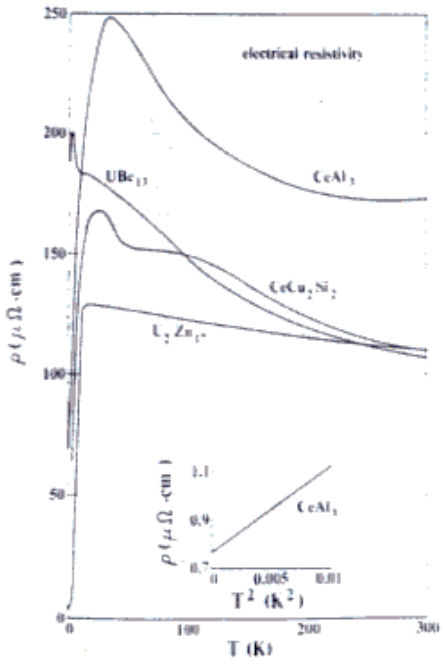

FIG. 3. The electrical resistivity as a function of temperature for the heavy-fermion systems U_2Zn_{17}, $CeAl_3$, $CeCu_2Si_2$, and UBe_{13}.

temperature in the heavy-fermion systems are summarized in Fig. 3. The large value of the resistivity and the often anomalous sign of its derivative are often attributed to the Kondo effect. Below room temperature, those heavy-fermion materials exhibiting the largest effective masses show an anomalous increase in the resistivity with decreasing temperature followed by a rapid decrease, which has been interpreted as the onset of "coherence" leading to the formation of the Fermi-liquid state. The temperature at which this occurs, the "coherence temperature," implies the existence of a characteristic energy scale, presumably the same energy scale inferred from the thermodynamic data. At low temperature, the resistivity of many heavy-fermion materials can be fitted by a form suggestive of strong quasiparticle-quasiparticle scattering,

$$\rho(T)=\rho_0+\rho_{ee}T^2, \tag{9}$$

where ρ_{ee} is some six to seven orders of magnitude larger than that observed in ordinary metals. The low-temperature resistivity of $CeAl_3$ displays a clear T^2 contribution as shown in the inset to Fig. 3. The resistivities of UPt_3, UAl_2, and YbBiPt do not display a maximum below room temperature but are still described by the Fermi-liquid form of Eq. (9) below a material-dependent temperature less than 10 K.

The resistivity is sensitive to impurities, pressure, and magnetic fields at low temperature, as discussed in detail by Ott and Fisk (1987) and Stewart (1984).

The frequency-dependent resistivity of UPt_3, $CeAl_3$, and $CePd_3$ has been measured in the microwave, infrared, and optical regions of the spectrum. At low frequency, the conductivity can be fitted by a Drude form,

$$\sigma(\omega)=\sigma(0)/(1+\omega^2\tau^2), \tag{10}$$

where $\sigma(0)$ is the dc conductivity, which is related to a relaxation time τ, a carrier density n, and an effective mass m^* by $\sigma(0)=ne^2\tau/m^*$. A narrow zero-frequency peak is observed at low temperatures; the relaxation time inferred from its width suggests that τ is enhanced compared to that for an ordinary metal by roughly the same factor as the effective mass that is obtained from thermodynamic properties. The narrow peak is not observed at room temperature, indicating that it is a signature of the heavy-fermion state. Complicated structure is observed at higher frequency, possibly due to interband transitions or plasmons.

In an ordinary metal, the Hall coefficient is weakly temperature dependent and provides information on the carrier charge and density. Experiments on the heavy-fermion systems find a strongly temperature-dependent Hall coefficient, as shown in Fig. 4. The Hall coefficient is large and positive at room temperature and increases with decreasing temperature. Usually the Hall coefficient displays a peak at nearly the same temperature as a similar feature in the resistivity. A peak is also observed in UPt_3 and UAl_2, which do not show an associated peak in the resistivity in the

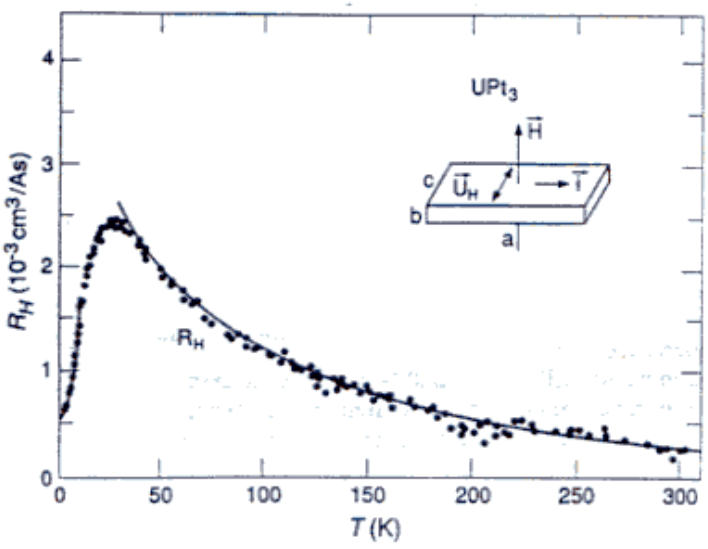

FIG. 4. The Hall coefficient as a function of temperature for UPt_3 measured in a 4-T field (from Schoenes and Franse, 1986). The solid line is a fit by the expression for incoherent magnetic scattering (see text).

corresponding temperature range. For metals containing small concentrations of impurity local moments, the Hall coefficient is often interpreted as the sum of an ordinary Hall coefficient, arising from the Lorentz force, and a generally large extraordinary term representing the incoherent scattering from local moments. At high temperature, this interpretation works well for the heavy-fermion systems (see solid line in Fig. 4) and is an aspect of the single-impurity phenomenology described below. In some heavy-fermion systems, the Hall coefficient changes sign at still lower temperatures. The rapid drop in R_H with temperature just below the peak has been interpreted as a signature of the onset of coherent scattering of the conduction electrons by the local f-atom moments.

1.2.6 Ultrasonic Measurements. The appearance of the heavy-electron state is evident in the temperature dependence of the elastic constants. Measurements on $CeAl_3$ (Lüthi, 1985), UPt_3, UBe_{13} (Yoshizawa *et al.*, 1985), and $CeCu_6$ (Weber, 1987) all show structure at low temperature and anomalies at high temperature, which contrast with the generally smooth and featureless elastic constants observed in an ordinary metal. Although some of these features signal structural phase transitions, as in the case of $CeCu_6$ at 220 K, others are interpreted as being due to magnetoelastic coupling to the crystal-field–split J multiplets (see Fulde *et al.* 1988). At low temperatures, where the heavy-electron state is developing, the temperature dependence of the elastic constants shows an anomalous change of slope for $CeCu_6$, UPt_3, and UBe_{13}.

The enormous density of states inferred from thermodynamic experiments suggests that the ultrasonic attenuation might be greatly enhanced. In fact, experiment finds that the magnitude of sound attenuation is of the order of that for an ordinary metal. In contrast to the comparatively smooth and featureless ultrasonic attenuation of an ordinary metal, an anomalous peak appears in UPt_3 at 12 K and in $CeCu_6$ at 2.5 K. In the latter case, the peak shifts to higher temperatures and broadens with increasing frequency. At still lower temperature, but above the superconducting transition, UPt_3 displays an attenuation that varies as T^2.

Specific-heat and resistivity data show that the coherent heavy-electron state is well developed at temperatures below ~ 10 K. In this regime, one expects that the phonon contribution to the ultrasonic attenuation should be negligible, and the energy of the sound wave should be dissipated primarily by the heavy-electronic liquid. As noted above, the ultrasonic attenuation is similar in magnitude to that measured for copper, which suggests that the electron-phonon coupling is reduced by an amount similar to the enhancement of the quasiparticle mass. In an ordinary metal, the sound speed v_s is much smaller than the Fermi velocity v_F, the electronic degrees of freedom are able to adjust rapidly to the lattice deformation presented by the sound wave, and the resulting attenuation process is isothermal. Lüthi (1985) pointed out that this is not the case in heavy-electron systems where $v_F \gtrsim v_s$, so that sound attenuation is adiabatic. As a consequence, the leading temperature dependence of the attenuation is due not only to the viscosity of the heavy-electron liquid, but also to the conduction of heat.

1.2.7 Nuclear Magnetic Resonance. At high temperature, the heavy-fermion systems show a nearly temperature-independent spin relaxation time T_1, consistent with the observed Curie-Weiss susceptibility. As the temperature is decreased, there is a regime below $\sim$ 10 K where T_1T is essentially constant (MacLaughlin, 1985), as expected for a Fermi liquid. As shown by Korringa, in a Fermi liquid the relaxation of polarization in the nuclear spin system is due to the coupling of the nuclear spin to the magnetic moment of the quasiparticles, so that $1/T_1T$ is proportional to the density of states at the Fermi surface (see Slichter, 1978). A comparison of T_1T for ^{13}Be in UBe_{13} and in $U_{0.967}Th_{0.033}Be_{13}$ just above T_c shows that $1/T_1T$ tracks the increase in γ observed in specific- heat experiments.

In URu_2Si_2, $T_1(T)$ decreases rapidly as the temperature is decreased through the antiferromagnetic transition at 17 K. It is interesting to note that a Korringa temperature dependence is evident above T_N and below $T \sim 10$ K.

1.2.8 Neutron Scattering. The results of inelastic neutron-scattering experiments on the magnetically ordered heavy-fermion systems U_2Zn_{17} and URu_2Si_2 and on the superconductor UPt_3 (see Aeppli *et al.*, 1988; Kjems and Broholm, 1988) show great similarities to

those systems such as $CeCu_6$ and $CeRu_2Si_2$ (see Rossat-Mignod *et al.*, 1988) that remain paramagnetic down to the lowest temperatures. All of these systems have a response function with a large q-independent component that can be fitted by a relaxational form,

$$\chi(q,\omega) = \chi_0\Gamma/(\Gamma - i\omega). \tag{11}$$

The systems also have a smaller q-dependent contribution that peaks at a nonzero q, indicative of antiferromagnetic correlations. As most of the integrated intensity expected from sum rules is tied up in the above response, there is little intensity left to assign to the low-ω and -q peak associated with Pauli paramagnetism. This implies strong spin-orbit coupling between the quasiparticles of a Fermi liquid, and that most of the response is of local origin.

In paramagnetic heavy-fermion systems, the antiferromagnetic correlations only become apparent at low temperatures. The widths of the peaks in $S(q,\omega)$ at fixed ω indicate correlation lengths of the order of 3–10 Å. In the ordered systems, the single-site component of the response function remains comparable to those of the paramagnetic systems, and the phase transitions are considered to be the result of a slight increase in the effective exchange interaction at low temperatures. This interpretation is consistent with the observation that many of the paramagnetic systems can be driven into the ordered phase with the introduction of impurities. It is surprising that of the ordered magnetic systems only URu_2Si_2 shows the existence of sharp spin-wave-like excitations, albeit with a small dispersion. Perhaps the most surprising result of all is found in the elastic scattering peaks: in URu_2Si_2 and UPt_3 the strength of the antiferromagnetic Bragg peak is indicative of an ordered magnetic moment with very small magnitude, $\sim 0.03\mu_B$ and $\sim 0.02\mu_B$, respectively. It should also be pointed out that the Bragg peaks are broadened, indicating finite correlation ranges in the ordered state, probably due to defects.

1.2.9 Photoemission. The photoemission spectrum provides a measure of the occupied portion of the electronic density of states, if surface effects and the interaction between the observed electron and the system can both be neglected. Likewise the inverse photoemission spectrum is related to the unoccupied electronic density of states. Using the phenomenon of resonance, it is possible to extract the f component from the spectra. The resulting spectra show marked distinctions between the normal rare-earth and actinide systems. On one hand, the cerium systems show pronounced features that may be attributable to transitions between localized ionic configurations. The energy separation between these features is taken to be a measure of U_{ff}, the Coulomb interaction energy between the electrons in the $4f$ orbitals on the cerium ions. On the other hand, normal uranium-based systems, such as UIr_3 (Arko *et al.*, 1983), agree quite well with band theory, indicating much smaller values of U_{ff} for uranium. This satisfactory state of affairs does not extend to the heavy-fermion uranium systems. When the $5f$ spectra of UPt_3 and UAl_2 were compared to the density of states obtained from band-structure calculations in the local-density approximation (Allen *et al.*, 1985), it was found that the observed spectra were considerably broader. Similar discrepancies were found for UBe_{13}, U_2Zn_{17}, and URu_2Si_2 (Allen , 1988). It has been shown that these discrepancies in width exhibit a systematic variation (Arko *et al.*, 1988) that is most profound in the heavy-fermion systems and is attributable to the development of satellites in the occupied portion of the spectra. Similar analysis of inverse photoemission experiments on UBe_{13} shows some evidence for the existence of satellites in the unoccupied $5f$ density of states. Thus, in the heavy-fermion systems it appears as though the spectrum may have slight features corresponding to localized states superimposed on top of a $5f$ band that cuts across the Fermi level.

In contrast to the uranium-based heavy-fermion systems, there have been very few high-resolution studies of cerium heavy-fermion systems. The earlier studies seem to indicate that the features seen in the f spectrum are less sharp than those found in the cerium systems with more modestly enhanced electronic masses, perhaps being more akin to the uranium heavy-fermion systems. The interpretation of the photoemission spectra of cerium-based compounds is the subject of considerable controversy (Allen *et al.*, 1986; Liu *et al.*, 1982; Freeman *et al.*, 1987). The spectra show three major peaks: one above, one below, and one cutting across the Fermi level. One school of thought attributes the peaks above and

below the Fermi level to transitions from an f^1 initial state to f^2 and f^0 final-state configurations, respectively. The peak near the Fermi level is associated with the Kondo effect whereby a spin polarization is induced in the conduction band at low temperatures, in order to compensate the magnetic moment of the f^1 configuration. The intensity in this peak is expected to scale with T_K, the characteristic energy scale of the Kondo model. A second school of thought attributes the existence of the two peaks at and below the Fermi level to two different mechanisms that are available to screen the charge deficiency associated with the f^0 final state. This school relates these screening channels to the systematic variation of the two peaks found in the photoemission of the praseodymium and neodymium rare-earth compounds, which have electronic mass enhancements of the order of those in ordinary metals.

1.3 Properties of the Superconducting State

Superconductivity in the heavy-fermion systems differs markedly from that in ordinary metals. Here, we briefly summarize some of the unusual properties of the heavy-fermion superconducting state, pointing out the differences between the heavy-fermion and conventional BCS superconducting states that lead to the conjecture that these are unconventional superconductors as defined in the Introduction.

At the transition temperature to the superconducting state T_c, the quasiparticles at the Fermi surface of a conventional superconductor are unstable to the formation of Cooper pairs. In the absence of a current, the Cooper pair consists of two electrons in states of momenta and spin $\mathbf{k},\sigma$ and $-\mathbf{k},-\sigma$ bound in a relative s-wave state by an attractive interaction mediated by phonons. Correlations between Cooper pairs generally lead to the formation of a gap in the quasiparticle dispersion relation,* which at sufficiently low temperature results in a thermally activated temperature dependence for specific heat, ultrasonic attenuation, nuclear spin relaxation, and thermal conductivity (see Schrieffer, 1964).

In contrast, the specific heat well below T_c for the heavy-fermion uranium compounds is described by

$$C(T)=\gamma_s T+\delta T^n \tag{12}$$

where γ_s is sample dependent and has often been attributed to conduction electrons that remain in the normal state, and n is 3 and 2 for UBe_{13} and UPt_3, respectively. Power-law temperature dependences have also been observed for ultrasonic attenuation, nuclear spin relaxation rates, thermal conductivity, and penetration depth. Sound attenuation in UPt_3 has been studied particularly thoroughly, and different exponents have been found, depending on the polarization and direction of propagation of the sound wave relative to the crystal axes. The exponents are also sample dependent. The power-law behavior observed in all of these properties strongly suggests that the gap function vanishes for some region on the Fermi surface and thus that, at the very least, the gap function depends strongly on the direction of $\mathbf{k}$. The more exciting possibility is that the gap function has a lower symmetry than does the crystal lattice as a result of quasiparticles that pair in a nonzero angular momentum state, possibly in a triplet state as in liquid ^{3}He.

The many-body wave function of the superconducting state is a phase-coherent superposition of single-particle states, and interference effects can be observed in many experiments. The attenuation of sound waves and the relaxation rate of a nuclear spin show classic signatures of interference effects in a conventional BCS superconductor (Schrieffer, 1964). As the temperature is lowered through the superconducting transition, sound attenuation decreases abruptly and the relaxation rate of a nuclear spin displays a Hebel-Slichter peak as shown for ^{119}In in Fig. 5(a). In the heavy-fermion systems, the Hebel-Slichter peak is not observed, as shown for UBe_{13} in Fig. 5(b); the spin relaxation rate drops abruptly below T_c. The ultrasonic attenuation, on the other hand, does not plummet below T_c but shows a sharp peak for UBe_{13} and for the best samples of UPt_3. A broader peak is evident for URu_2Si_2.

We have already observed that the specific-heat discontinuity is a large fraction of the

*This does not occur in so-called gapless superconductors where the gap has been suppressed by impurities. The heavy-fermion superconductors are not intrinsically gapless.

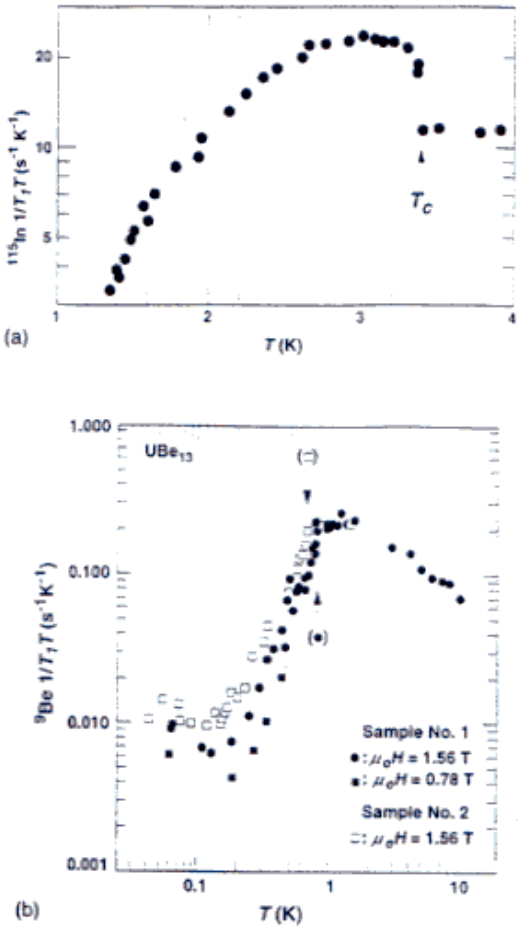

FIG. 5. Nuclear spin relaxation rate for (a) the conventional BCS superconductor ^{115}In and (b) the heavy-fermion system UBe_{13}. Note the absence of a Hebel-Slichter peak in UBe_{13}.

specific heat at T_c, consistent with the expectation for quasiparticles with a large effective mass condensing into the superconducting state. The normalized specific-heat discontinuities $\Delta C(T_c)/C_N(T_c)$ of several heavy-fermion superconductors are listed in Table 5. For most superconductors, $\Delta C(T_c)/C(T_c)$ lies within 20% of the weak-coupling BCS theory result of 1.43 (Parks, 1969). Larger values may occur as a result of strong coupling to lattice phonons. With the exception of UBe_{13} and $CeCu_2Si_2$, the heavy-fermion superconductors show substantially smaller normalized specific-heat discontinuities. Moreover, the transition is often broad, as in UPt_3 and URu_2Si_2. We return to this point below.

The heavy-fermion superconducting state is very sensitive to impurities and defects. The transition temperature can be strongly depressed in UPt_3 by grinding the sample. The substitution of a small amount of thorium for uranium in UBe_{13} leads to a rapid decrease of T_c. Further thorium substitution reveals the complicated phase diagram of $U_{1-x}Th_xBe_{13}$ in Fig. 6 that shows at least two and possibly more superconducting phases. For thorium concentrations lying roughly between 0.017 and 0.05, two phase transitions were observed in specific-heat experiments with discontinuities at the transitions of comparable size. The upper critical field of the higher-temperature phase behaves differently from that for pure UBe_{13} when doped with small amounts of Gd impurities, suggesting that these are two different superconducting phases. Early sound attenuation experiments suggested that the low-temperature phase transition was to a magnetically ordered state. Subsequent neutron-scattering experiments failed to observe a magnetically ordered state. Muon-spin resonance experiments detect a small ordered moment $\lesssim 0.01\mu_B$. The small size of the moment suggests the possibility that the low-temperature transition may separate two unconventional superconducting phases. We discuss this possibility in Sec. 3 below.

The phase diagram of a conventional superconductor is determined by the ratio of the characteristic length scale over which the magnetic field varies, the penetration depth λ,

Table 5. Properties of some heavy-fermion superconductors.

Compound	T_c (K)	$\Delta C(T_c)/C(T_c)$	$-dH_{c2}/dT\|_{T\sim T_c}$ (T/K)	$H_{c2}(T=0)$ (T)
$CeCu_2Si_2$	~0.7	1.3	23	2.0
UBe_{13}	0.85	2.5	42	8
UPt_3	0.45	1.0	6.4/7.5	2.0/2.5
URu_2Si_2	1.1	0.82	4/14	8.0/2.0
UPd_2Al_3	2.0	1.2	4.3	~3.6

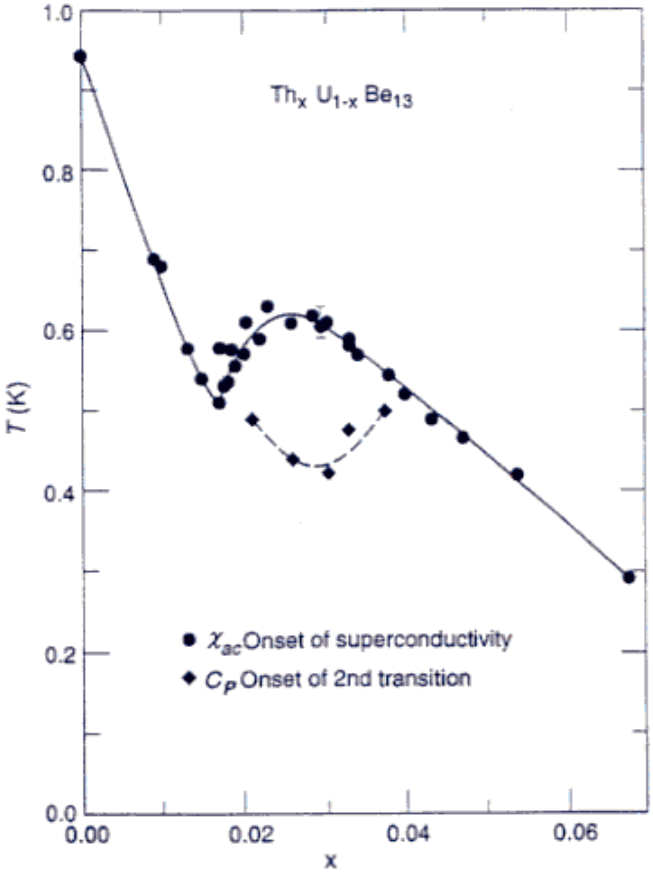

FIG. 6. The temperature–thorium concentration (x) phase diagram of $U_{1-x}Th_xBe_{13}$. Note the striking change in $T_c(x)$ (solid line) as x is increased through $x_c \simeq 0.018$ and the second phase transition at $T_{c2}(x)$ (dashed line).

to that over which the order parameter varies, the coherence length ξ. For a type-II superconductor, $\kappa = \lambda/\xi > \sqrt{2}$, and the H-T phase diagram shows two superconducting phases and one normal phase separated by the lower critical field $H_{c1}(T)$ and the upper critical field $H_{c2}(T)$. In the Meissner phase ($H < H_{c1}$), magnetic fields are excluded from the superconductor. As the field is increased above H_{c1}, magnetic flux penetrates the superconductor in a triangular lattice of flux tubes. Each flux tube is a vortex in the phase of the order parameter. The order parameter vanishes on the vortex axis and heals to its bulk equilibrium magnitude in a distance of the order of ξ. The magnetic field is a maximum at the center of the vortex and decays on the scale of λ. As the field is increased so too is the density of vortices until at H_{c2} the vortex cores begin to overlap and a transition occurs to the normal state.

The heavy-fermion superconductors are type-II superconductors with κ, as inferred from the slopes of H_{c2} and H_{c1} at T_c, as large as ~ 50 or more. These rank among the largest κ values found in conventional superconductors, for which the large value of κ occurs as a result of scattering from impurities. In contrast, the heavy-fermion substances are pure materials. The temperature dependence of $H_{c2}(T)$ for the heavy-fermion systems is generally unusual. As shown in Table 5, $dH_{c2}(T)/dT|_{T_c}$ for UBe_{13} is unusually large, possibly exceeded only by that for the high-T_c superconductors. In UBe_{13}, $H_{c2}(T)$ is nearly linear over a large range of temperature and shows a change in slope at about 0.5 K. In UPt_3 an anomalous crossover in the anisotropy of $H_{c2}(T)$ occurs with decreasing temperature. For temperatures near T_c, $H_{c2\parallel}/H_{c2\perp} \sim 1.3$ (where $\parallel$ and $\perp$ refer to the field direction with respect to the crystal c axis) and drops to

~ 0.8 as T approaches 0. The $T=0$ extrapolated value of H_{c2} exceeds simple estimates of the paramagnetic limit at which the spin-polarized normal state is favored over a conventional superconducting state. The upper and lower critical fields in the basal plane of UPt_3, and $H_{c1}(T)$ in $U_{1-x}Th_xBe_{13}$ at the low-temperature transition, show unusual sharp kinks.

The phase diagram of UPt_3 in the H-T plane shows five superconducting phases in contrast to the two observed in an ordinary superconductor. This is strong evidence, as we discuss below, that UPt_3 is an unconventional superconductor. The phase diagram as observed in the sound speed measurements of Adenwalla *et al.* (1990) is shown for field in the basal plane and along the c-axis in Fig. 7 (see also Bruls *et al.*, 1990). The figure shows three phases in the mixed state, but does not show the Meissner phases, which lie close to the temperature axis.

A connection between weak antiferromagnetic order and superconductivity is suggested in Table 1. For some of the heavy-fermion superconductors, a transition to an antiferromagnetic state with an extraordinarily small magnetic moment, of order $\sim 0.01\mu_B$, occurs at a Néel temperature $T_N \sim 10T_c$. A notable example is UPt_3, for which recent specific-heat (Fisher *et al.*, 1989) and sound-velocity experiments observe two superconducting transitions 60 mK apart, which may be a signature of the coupling of an unconventional superconducting-order parameter to a magnetic-order parameter (see Sec. 2.3 and Hayden *et al.*, 1992). It is interesting that prior experiments found only a single broad peak at the superconducting transition in UPt_3 as also observed for URu_2Si_2. This suggests that an aging effect may occur in UPt_3 and that antiferromagnetic order may appear with time (Smith, 1992). A possible mechanism for an aging effect is radiation damage due to uranium decay.

2. THEORY

2.1 Phenomenology

2.1.1 Landau Fermi-Liquid Theory. At low temperature, the linear dependence of the specific heat, the nearly temperature-independent susceptibility, and the large T^2 coefficient of the resistivity suggest that the heavy-fermion systems settle into a strongly renormalized Fermi-liquid state below a (material-dependent) characteristic temperature. Well

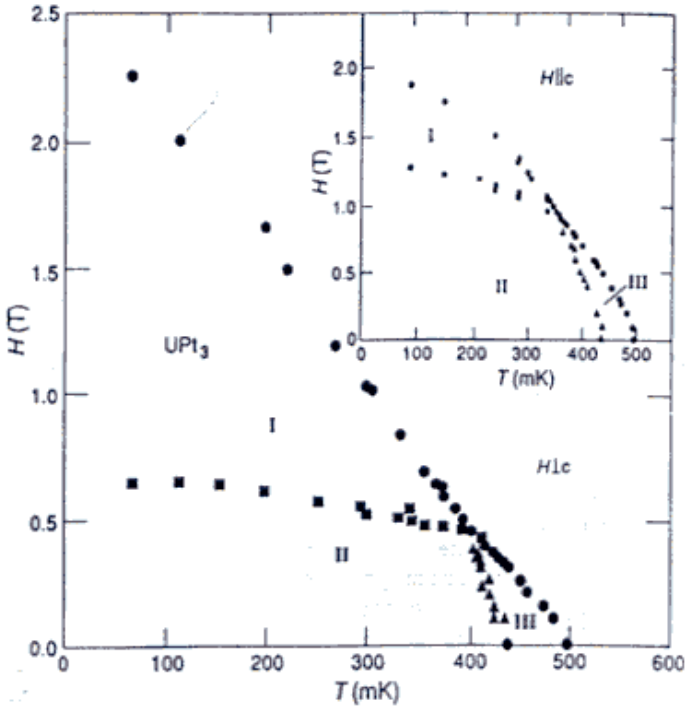

FIG. 7. The field-temperature phase diagram of the superconductor UPt_3 as deduced from sound-velocity measurements for fields in the basal plane (from Adenwalla *et al.*, 1990). The lower critical field separating the mixed phases from the Meissner phases is not shown but lies just above the temperature axis. In all there are five superconducting phases in the H-T plane. Inset: The corresponding phase diagram for fields along the c axis.

below an effective degeneracy temperature, the properties of diverse systems of strongly interacting fermions resemble those of a system of noninteracting fermions and are determined in large part by the low-energy excitations of the interacting system. The phenomenological Fermi-liquid theory of Landau may be used to describe such systems. The central concept of Landau Fermi-liquid theory is the quasiparticle, which is an elementary excitation of the interacting system that can be crudely viewed as a particle surrounded by a cloud of other particles. The lifetime of a quasiparticle near the Fermi energy [varying as $1/(\epsilon^2+\pi T^2)$, with ϵ measured from the Fermi energy ϵ_F] is sufficiently long to provide a useful description of the low-lying elementary excitations of the interacting system. The original system of strongly interacting "bare" particles is thought of as a system of interacting quasiparticles. The dynamical properties of these quasiparticles, such as the mass, are renormalized from those of the bare particles by the accompanying motions of the surrounding particle clouds. The Landau theory provides no prescription for calculating the properties of or interactions between quasiparticles; rather, these are to be determined from experiments or microscopic theories. The Landau theory provides relations between physical quantities in terms of the effects of residual screened interactions between the quasiparticles. A proper Landau theory for any metal should incorporate the symmetry of the underlying crystalline lattice as outlined by Fulde *et al.* (1988) for heavy-fermion systems. Such a description is complicated by the occurrence of a large number of parameters describing the quasiparticle interactions. So we describe an overly simplified theory that is similar in construction to the Fermi-liquid theory for liquid ^{3}He, for the purpose of introducing Fermi-liquid theory and also because the results of some calculations based on model Hamiltonians are expressed in terms of the Landau parameters of this model.

The free energy may be expanded about its zero-temperature limit in terms of the interactions between quasiparticles,

$$F(T)=F(0)+\sum_{\mathbf{p}} E^0_{\mathbf{p}}\delta n^{\sigma}_{\mathbf{p}}+\sum_{\mathbf{p},\mathbf{p}',\sigma,\sigma'} f^{\sigma,\sigma'}_{\mathbf{p},\mathbf{p}'}\delta n^{\sigma}_{\mathbf{p}}\delta n^{\sigma'}_{\mathbf{p}'} + \text{terms } O((\delta n)^3), \tag{13}$$

where $\mathbf{p}$ and σ are momentum and spin variables and $\delta n^{\sigma}_{\mathbf{p}}$ is the deviation of the distribution function from its zero-temperature limit. We have retained only the interaction between two quasiparticles $f^{\sigma,\sigma'}_{\mathbf{p},\mathbf{p}'}$, which is dominant at sufficiently low temperature. Symmetries are used to simplify the form of f and to choose an appropriate set of basis functions; the coefficients appearing in the basis function expansion are the so-called Landau parameters. For example, rotational symmetry in spin space leads to the form $f^{\sigma,\sigma'}_{\mathbf{p},\mathbf{p}'}=\mathbf{1}f^{s}_{\mathbf{p},\mathbf{p}'}+\boldsymbol{\sigma}\cdot\boldsymbol{\sigma}'f^{a}_{\mathbf{p},\mathbf{p}'}$. For liquid ^{3}He, the appropriate basis functions are the usual spherical harmonics; $\mathbf{p}$ has the meaning of a quasiparticle momentum and σ the meaning of a quasiparticle spin. Various thermodynamic and transport properties of the system can be expressed in terms of the Landau parameters. In this case one finds for the compressibility

$$\chi_d=\frac{m^*/m}{1+F^s_0}\chi^0_d, \tag{14}$$

and for the susceptibility

$$\chi_s=\frac{m^*/m}{1+F^a_0}\chi^0_s, \tag{15}$$

where χ^0_d and χ^0_s are the corresponding susceptibilities in the noninteracting system, and the dimensionless Landau parameter $F^{\lambda}_l=N(\epsilon_F)f^{\lambda}_l$, where $N(\epsilon_F)$ is the density of states that appears in the linear coefficient of the specific heat,

$$\gamma=\frac{\pi^2}{3}N(\epsilon_F)k_B^2=\frac{m^*}{m}\gamma^0, \tag{16}$$

m^* is the quasiparticle effective mass, and k_B is Boltzmann's constant.

Carneiro and Pethick (1975) showed that long-wavelength fluctuations of spin and density in a system of interacting fermions will generally contribute a term to the low-temperature specific heat that depends logarithmically on the temperature,

$$C(T)=\gamma T+\zeta T^3\ln T+\beta T^3+\ldots, \tag{17}$$

where ζ may be expressed in terms of the Landau parameters.

The observation that UPt_3 has a specific heat of the form Eq. (17) led to the proposal that quasiparticle spin fluctuations play a similar role in UPt_3 as they do in ^{3}He (Stew-

art, 1984). The electron-phonon interaction can also contribute to the $T^3 \ln T$ term in the specific heat, but the sign of this contribution to ζ is opposite to that produced by the spin and density fluctuations and is also of opposite sign to that observed in UPt_3. A single-band spin-$\frac{1}{2}$ model was developed for UPt_3 and UAl_2, assuming an expression for ζ taken from the Landau theory of ^{3}He, estimating the effective radius of the Fermi surface, and neglecting scattering processes involving angular momentum channels of $l=2$ and higher (see Pethick and Pines, 1987, for a review). This allowed the analogy of UPt_3 and ^{3}He to be extended to the superconducting state. In ^{3}He the superfluidity is believed to occur due to an attractive interaction mediated by spin fluctuations. The analogy yields an attractive effective interaction between two electrons, which produces superconductivity below a critical temperature T_c. They calculated the pressure dependence of T_c and found it to be in agreement with experiment. The mechanism for the formation of Cooper pairs (see Sec. 3) in this model is of purely electronic origin, and the resulting superconducting state is unconventional. A further consequence of this model is that the effective moments of the quasiparticles are renormalized so that $\mu < \mu_B$.

2.1.2 Single-Impurity Model. For temperatures well above the "coherence temperature" T^*, the single-impurity Anderson model provides a useful phenomenological framework for the heavy-fermion systems. This model was originally introduced by Anderson to describe dilute magnetic impurity ions dissolved in a solid. However, the heavy-fermion systems have a relatively high concentration of magnetic (f) ions, and so the use of this single-ion phenomenology in the high-temperature regime implicitly assumes the decoupling of the f orbitals on different lattice sites.

The single-ion Anderson model describes a doubly degenerate localized level, e.g., an f level, that is bathed in a Fermi sea of conduction electrons. The Hamiltonian can be written as

$$H = H_f + H_d + H_{fd} , \tag{18}$$

where H_f describes the f-electron system, H_d describes the conduction-electron system, and H_{fd} describes the coupling between these systems. The Hamiltonian H_f is

$$H_f = \sum_{\alpha} E_f n_\alpha + \sum_{\alpha > \beta} U_{ff} n_\alpha n_\beta , \tag{19}$$

where n_α represents the number of electrons in the f orbital with spin index α. The first term, proportional to E_f, represents the binding energy of an electron of spin α in the f shell. The second term, proportional to U_{ff}, represents the Coulomb repulsion between pairs of electrons in the f shell. The Pauli exclusion principle makes this term inactive when $\alpha = \beta$. The conduction electrons described by H_d are noninteracting conduction electrons in band states:

$$H_d = \sum_{\mathbf{k}\alpha} e_{\mathbf{k}} n_{\mathbf{k}\alpha} , \tag{20}$$

where $n_{\mathbf{k}\alpha}$ is the number of electrons of spin α in the conduction-band state labeled by the Bloch wave vector $\mathbf{k}$ and $e_{\mathbf{k}}$ is the dispersion relation of the conduction-band states. The f- and d-electron systems are coupled by a spin-conserving hybridization interaction H_{fd}, which represents processes whereby individual electrons can tunnel out of the f level into the conduction-band states along with the reverse processes. This hybridization process has matrix elements between localized f states $|f\alpha\rangle$ and itinerant states $|d\mathbf{k},\alpha\rangle$ given by

$$V_{\mathbf{k}} = \langle f\alpha | H_{fd} | d\mathbf{k},\alpha \rangle . \tag{21}$$

Applying Fermi's "golden rule," one obtains an effective f-level width Δ, for the state in which the f electron is occupied by a single electron, given by

$$\Delta = \pi |V|^2 N(e_F), \tag{22}$$

where $N(e_F)$ is the conduction-band density of states, per spin, evaluated at the Fermi energy e_F.

One question of interest is whether the impurity ion can carry a magnetic moment in a metallic matrix. Anderson (1961), working within the Hartree-Fock approximation, showed that a magnetic moment might be formed for sufficiently large U_{ff}/Δ, whereas for smaller values of the ratio the impurity was nonmagnetic. These results can be understood by first considering two extreme limits that can be solved exactly: In the atomic limit, for which $\Delta = 0$, adding an electron of spin β to a localized level already occupied by an

electron of spin α costs an energy of $E_f + U_{ff}$, whereas the energy for removing the electron of spin α is E_f. Thus, the one-electron density of states is split into two sharp levels; the β level occurs above the Fermi level, and the α sublevel occurs below the Fermi level. The other extreme limit is the noninteracting limit where $U_{ff} = 0$, in which case the f states admix with the conduction-band states through the hybridization term, giving rise to a resonant peak in the f density of states at E_f with width given by Δ. In this noninteracting case, the f states of spin α and spin β are occupied by equal numbers of electrons (possibly fractionally) and hence possess no net magnetic moment. For the same reason that the f level splits in the atomic limit, the Hartree-Fock solution also shows a splitting of the f density of states for large but finite values of the ratio U_{ff}/Δ. The two subbands are of different spin characters and are separated by an energy of the order of U_{ff}. This split density of states, shown in Fig. 8, can lead to the formation of a local f moment when occupied by electrons in accordance with the Pauli exclusion principle. For systems with a number of f electrons per f ion less than unity, $n_f < 1$, the Hartree-Fock treatment requires that $|E_f - e_F| < \Delta$, which places the lower subband close to the Fermi level and the upper subband above. For almost integer occupation of the f level the lower subband will lie at even lower energies and may have very little weight at the Fermi energy. This

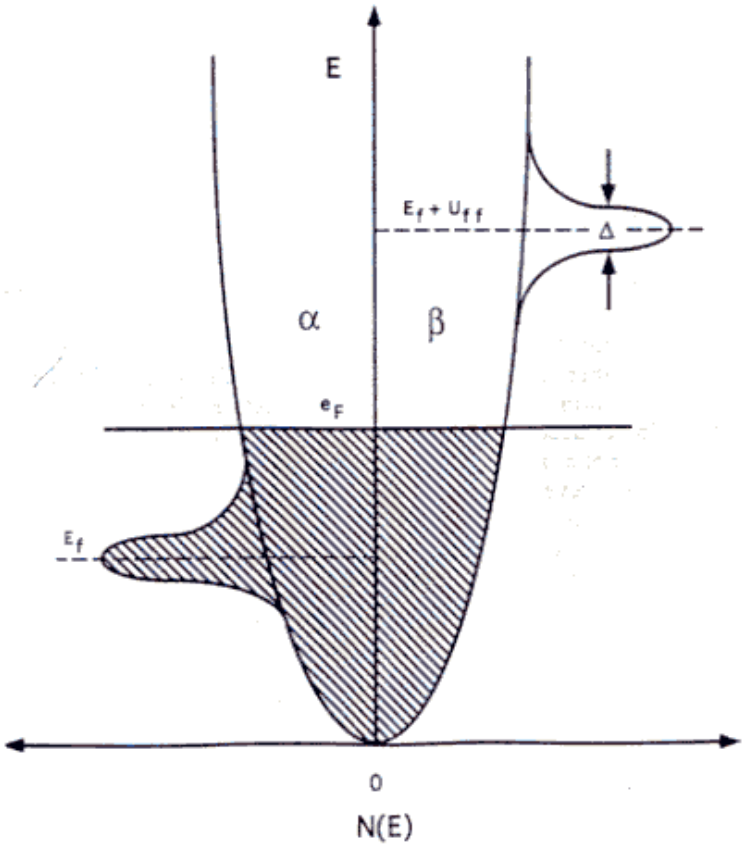

FIG. 8. The density of states from the Hartree-Fock solution to the single-impurity Anderson model showing that the effect of the intra-atomic Coulomb interaction is to split the original f level into two levels according to spin. One level occurs at the position of the original f level, the other at an energy U_{ff} higher and above the Fermi energy. Processes by which an electron can tunnel from an atomic f orbital to the conduction band and the reverse processes called hybridization are responsible for the finite level width $\sim\Delta$.

latter regime is defined as the Kondo regime, in which Hartree-Fock theory would predict well-developed local moments. Schrieffer and Wolff (1966) have shown that these local moments are coupled to the spin polarization of the conduction electrons by an antiferromagnetic exchange interaction of strength $J=V^2/E_f$. This coupling introduces quantum fluctuations in the directions of the local moments that are not included in the Hartree-Fock solution.

The most marked modifications to the Hartree-Fock results are required in the Kondo regime, as is suggested by renormalization-group scaling arguments (Haldane, 1978). What happens is that J produces a bound state that when occupied by an electron produces a compensating spin polarization in the conduction electrons. At low temperatures the resulting complex is a spin singlet, whereas at higher temperatures the bound state is ionized leading to the reappearance of the local moment. This low-energy behavior leads to the appearance of a narrow temperature-dependent resonance in the single-electron spectrum at the Fermi level known as the Kondo peak. Nozières (1974) has shown that the low-temperature properties can be described quite well by a Landau Fermi-liquid theory in which the impurity produces a phase shift for the conduction electrons that reaches $\delta_0(\mathbf{k}_F)=\pi/2$ at the Fermi energy. The picture of a low-energy, low-temperature Fermi liquid can also be obtained by a projection method for minimizing the Coulomb interaction energy, developed by Gutzwiller (1965), which basically renormalizes the hybridization width Δ by a factor of $1-n_f$ corresponding to the elimination of processes in which an electron may hop into an f shell that is already occupied. For cerium, with an f band less than half filled, the maximum intensity in the Kondo peak is above the Fermi energy. The resulting picture of the one-electron spectrum in the Kondo regime is that of a filled subband below the Fermi energy, separated by an energy U_{ff} from an unfilled upper subband, together with a temperature-dependent Kondo resonance located at the Fermi energy. The width of the Kondo resonance is related to the Kondo temperature T_K where $k_B T_K \sim \Delta(1-n_f)$ and its peak height is $\sim 1/\pi\Delta$.

Confidence in the above picture has been established by exact Bethe-*Ansatz* solutions (Schlottmann, 1989; Tsvelick and Wiegman, 1983) and by exact numerical renormalization-group studies (Krishnamurthy *et al.*, 1980). One of the most notable features of these solutions is that the thermodynamic properties only depend on a single energy scale given by the Kondo temperature.

For the heavy-electron systems, one imagines a lattice of such impurities (the cerium or uranium atoms). As the temperature is reduced it is possible that the compensating polarization clouds of each impurity lock together in a coherent heavy-fermion state. This possibility has motivated studies of the interactions between two Anderson impurities (Jones *et al.*, 1988). As a result of the occurrence of another energy scale, the exchange interaction J between the impurity moments, two possibilities arise. If $J \ll T_K$, then the compensation of each local moment occurs independently, whereas if $J \gg T_K$, the moments order before the screening clouds develop.

Nozières (1985) noted another complication of this picture. The formation of a compensating screening cloud only involves conduction electrons within T_K of the Fermi surface, but the total number of such electrons is much less than that required to screen every local moment in a concentrated compound.

Although much use can be made of the above phenomenologies, it remains unclear to what extent they provide a firm theoretical basis for understanding the properties of a lattice of f ions immersed in a Fermi sea of conduction electrons.

2.1.3 Model Hamiltonians. It is believed that the physics of the single Kondo impurity is related to the physics of the process by which the system of apparently weakly interacting local moments in a sea of conduction electrons is transformed to an itinerant band of heavy quasiparticles. The Anderson lattice model makes this notion more precise and quantitative, by generalizing the Hamiltonian of a single f impurity to a dense lattice of f sites.

The Anderson lattice Hamiltonian may be written as the sum of three terms as in Eq. (18), but with H_f representing a lattice of f ions:

$$H_f = E_f \sum_{i\alpha} n_{f\alpha i} + \sum_{i,\alpha<\beta} U_{ff} n_{f\alpha i} n_{f\beta i} , \qquad (23)$$

where i labels the f-lattice sites and α labels an appropriate basis set that reflects the full 14-fold spin- and orbital-degenerate f level. The hybridization terms are generalized by allowing the f level at each site to admix with the conduction-band states. The transformation from the Wannier representation of the f levels to a Bloch representation,

$$|f\mathbf{k},\alpha\rangle = \frac{1}{\sqrt{N_s}} \sum_i e^{i\mathbf{k}\cdot\mathbf{R}_i} |fi,\alpha\rangle, \tag{24}$$

together with conservation of crystal momentum, leads to the simple form for the hybridization matrix element

$$V_{\mathbf{k}} = \langle f\mathbf{k},\alpha | H_{fd} | d\mathbf{k},\alpha\rangle. \tag{25}$$

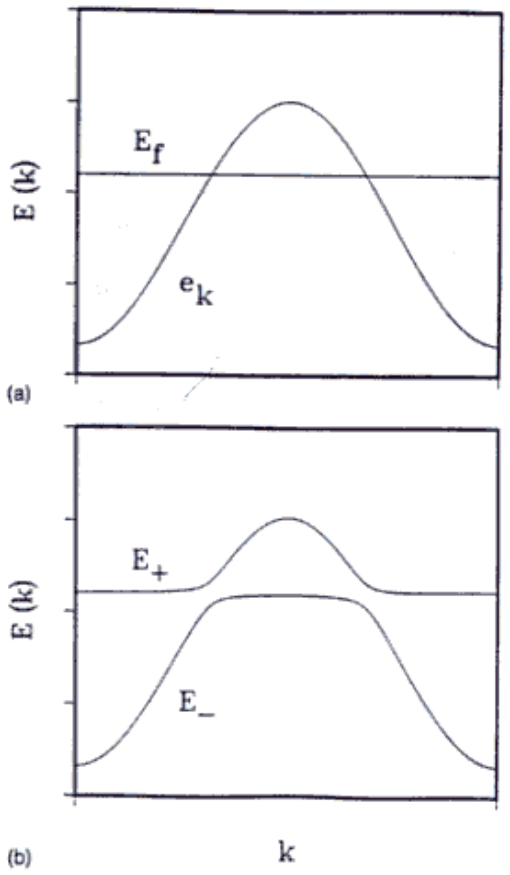

FIG. 9. Flat atomic f level, and a broad conduction band shown as a function of crystal momentum in (a), are admixed by the hybridization matrix element $V_{\mathbf{k}}$ to produce the two spin-degenerate bands shown in (b).

In the absence of the intrasite Coulomb interaction, $U_{ff} = 0$, the lattice Hamiltonian can be completely diagonalized. This yields two spin-degenerate bands with dispersion relations

$$E_{\pm}(\mathbf{k}) = \tfrac{1}{2}[E_f + e_{\mathbf{k}} \pm [(E_f - e_{\mathbf{k}})^2 + |2V_{\mathbf{k}}|^2]^{1/2}], \tag{26}$$

which are sketched in Fig. 9. If the hybridization matrix element $V_{\mathbf{k}}$ is non-vanishing over the entire Brillouin zone, then the electronic-spectrum exhibits an indirect gap of magnitude V^2/W where W is the d-band width. The existence of a hybridization gap depends on the validity of many simplifying assumptions such as the neglect of direct f-f hopping, crystalline field effects, spin-orbit coupling, and so on. Nonetheless, the hybridization gap often plays an important role in many-body theories for the heavy-fermion semiconductors.

The introduction of the Coulomb interaction U_{ff} is expected to modify the above simple picture of the electronic states. Unfortunately, no exact solutions for the Anderson lattice model are known, leading researchers to rely on approximate methods.

At high temperature, the Anderson lattice Hamiltonian is expected to behave like an incoherent superposition of single Anderson impurities. As observed above, the properties of the heavy-electron systems at high temperature resemble those of a collection of single Anderson impurities in the Kondo regime. Thus one expects that in order for the Anderson lattice Hamiltonian to describe the heavy-fermion systems, the ratio U_{ff}/Δ should be large and the f level should lie well below the Fermi level. Moreover, the upper single-impurity band, $E_f + U_{ff}$, lies well above the Fermi level. In this situation, fluctuations of the f-site charge are strongly suppressed and fluctuations of the f-site moments are the important degrees of freedom.

Many different approximations have been developed for the Anderson lattice Hamiltonian, as reviewed by Lee *et al.* (1986) and Fulde *et al.* (1988). Of particular interest for the heavy-fermion systems are strong-coupling approximations that include direct decoupling of the hierarchy of equations of motion for the Green's functions, variational methods (Rice and Ueda, 1985), and expansions in powers of the spin and orbital degeneracy of the f levels, which are generalizations

to the lattice of methods used for the single-impurity problem known as $1/N$ expansions. The decoupling schemes and variational methods, depending on initial choices of allowable physical states, are not systematic and have not been the methods of choice for most researchers. For technical reasons, much of the work on the Anderson lattice Hamiltonian (e.g., $1/N$ expansions) has been done for the limit $U_{ff} \to \infty$ in the hope of describing the essential features of strong correlations.

The expansions in powers of the spin-orbital degeneracy N are made with the assumption that N is a large number and that the expansion is rapidly convergent (Bickers 1987; Newns and Read, 1987). In the limit $N \to \infty$, a mean-field solution is expected to be exact. This mean-field solution produces a set of bands similar to those shown in Fig. 9(b). However, the position of the f level is renormalized upwards, and the magnitude of the hybridization is reduced in order to minimize the Coulomb interaction energy. Physically, the smaller the number of f electrons, the less the interaction energy. Furthermore, reducing the hybridization matrix element from its noninteracting value makes it less likely for a conduction electron to hop into a localized f orbital and interact with the electrons already present there, which also minimizes the effects of the Coulomb interaction. The above picture is that of renormalized bands, in which the width of the f states is narrowed by the Coulomb interactions. This picture is modified by including terms of higher order in $1/N$. In general, the above states are subject to further changes in their dispersion relations and also acquire a finite lifetime that is both temperature and energy dependent. The energy dependence of the lifetime can cause structure in the electronic density of states that is not directly related to the quasiparticle dispersion relations. For physical values of N, the contribution of the quasiparticle dispersion relations to the density of states is a small peak close to the Fermi energy, and the main structure occurs as a result of the energy dependence of the lifetime.

Many results obtained by the $1/N$ expansion technique can also be obtained by other methods. An example is a variational scheme based on a method of projecting out doubly occupied f states, thereby minimizing the energy of the Coulomb interaction. Rice and Ueda (1985) applied this method to the Anderson lattice model and produced an effective band model similar to that obtained by the $1/N$ expansion techniques. These authors argued that in the Kondo regime the physics should be similar to that of the Hubbard model near localization. The main results are discussed in the Landau Fermi-liquid language introduced above. They find that the divergence of the effective mass, as localization is approached, is balanced by a similar divergence in F_0^s, and thus the charge susceptibility remains unrenormalized. The parameter F_0^a that controls the tendency for magnetic ordering depends strongly on the total degeneracy of the f level. In the direct $1/N$ expansion techniques it has been found that the paramagnetic heavy-fermion state is only stable if the orbital degeneracy is large.

Although the strength of the Coulomb interaction is sufficiently large that series expansions in powers of U_{ff} are not expected to converge rapidly, studies along these lines have been pursued (Czycholl, 1986). The main motivation for applying perturbation theory to the Anderson lattice model is that for the single-impurity Anderson model with particle-hole symmetry ($2E_f + U_{ff} = 2e_F$; see Fig. 8), perturbation expansions for certain quantities are rapidly convergent (Horvatić and Zlatić, 1985). Since the heavy-fermion state itself is apparently a Fermi liquid and the formal underpinnings of Fermi-liquid theory are described in terms of self-consistent perturbation theories that sum infinite classes of diagrams, it is further hoped that such an approach could at least describe the low-temperature limit. Numerical calculations are required to evaluate the expressions of self-consistent perturbation theories beyond Hartree-Fock theory, and it is possible to include the results of band-structure calculations without further approximation. The choice of classes of diagrams to be summed is to some extent arbitrary, although conservation laws provide guidance in selecting sets of terms. Apparently because of the difficulty of the numerical calculations (Schweitzer and Czycholl, 1990), fully self-consistent calculations have not been reported for the Anderson lattice model in three dimensions; the calculations that have been performed have been limited to second-order perturbation theory. The results show that the quasiparticle dispersion relation is strongly renormalized near the Fermi energy and that a temperature-

dependent peak appears in the density of states at the Fermi level that bears a qualitative resemblance to the Kondo resonance in the single- impurity model. An unfortunate feature of these calculations is that they have been performed largely for models that include only one spatial dimension; such models may contain well-known pathologies related to low dimensionality.

Both the weak-coupling and strong-coupling schemes do yield results that have some qualitative similarities, namely a narrow temperature-dependent peak in the density of states close to the Fermi energy. However, no quantitative agreement has been reached between the strong- and weak-coupling schemes. This has led various groups to apply numerical techniques, which have given some insight into these problems. Conspicuous among these is the quantum Monte Carlo method, which has allowed the accuracy of some approximate solutions to be assessed. Unfortunately these calculations have been restricted to small systems, high temperatures, and near particle-hole symmetry. Thus, despite its deceptively simple appearance, the exact solution for the low-temperature, low-energy properties of the Anderson lattice Hamiltonian remains elusive.

2.2 Electronic Structure Calculations

The electronic structures of the heavy-fermion systems $CeAl_3$, $CeCu_2Si_2$, $CeCu_6$, UBe_{13}, UPt_3, U_2Zn_{17}, and URu_2Si_2 have all been calculated in the local-density approximation (Fulde *et al.*, 1988). This approach is based on a theorem due to Kohn and Sham (1965) that states that the energy of the fully interacting electronic system is a functional of the electronic density (see ELECTRON STATES IN SOLIDS). Electronic correlations are incorporated by the introduction of an exchange and correlation term in the energy functional, and the result of the calculations should be the exact real-space electronic charge density and the total energy. The exact form of the exchange and correlation functional is unknown, but in the local-density approximation (LDA) it is approximated by the form appropriate for a system with uniform electron density, but evaluated with the local value of the electronic density. As a by-product of the Kohn-Sham formalism a set of eigenfunctions and eigenvalues is generated; the spectrum of eigenvalues often exhibits a close resemblance to the electronic spectrum, as measured by, for example, angle-resolved photoemission. An advantage of these calculations is that crystal-field effects and spin-orbit interactions are automatically included. In the latter case, fully relativistic calculations are required. The results of these calculations share the common feature of a band with primarily f character straddling the Fermi energy. For cerium systems, the occupied $4f$ weight accounts for 1 to 1.3 f electrons, whereas for the uranium systems, the $5f$ count lies between 2 and 3 electrons per uranium atom. The total f bandwidths are of the order of 1 eV as the f character admixes to states in bands that are energetically removed from the Fermi energy. Although this is narrow when compared to the bandwidth of a typical conduction band, it is still too large to account for the order-meV energy scale deduced from the thermodynamic and transport properties of the heavy-fermion materials. Moreover, the calculated total density of states at the Fermi energy is still much smaller than that deduced from the linear temperature coefficient of the specific heat.

A tight-binding parametrization of LDA calculations is essential, if quantitative predictions incorporating many-body correlations are to be made; only a few such parametrizations have been performed. Although the entire parameter sets may vary from one fitting procedure to the next, the individual parameters do indicate the importance of hybridizing the f band with non-f bands.

2.3 Superconductivity

Perhaps the most exciting aspect of the heavy-fermion systems is that some of them might be unconventional superconductors. Various authors have proposed that an anisotropic but still conventional state occurs as a result of the strong coupling of f electrons to the lattice. This point of view is reviewed at length in Fulde *et al.* (1988).

The superconducting state is expected to be unusual at the very least. The standard theory of superconductivity relies in large part on the existence of small parameters. The difference in the thermodynamic potential between the superconducting state and normal state may be expressed as an asymptotic expansion in

T_c/T_F, where T_F is the Fermi energy. The leading term is of order $(T_c/T_F)^2$ and gives the weak-coupling BCS theory of superconductivity, which can allow both conventional and unconventional order parameters. Eliashberg theory, which treats strong electron-phonon coupling, is of order $(T_c/T_F)^2$ and also of leading order in the ratio of the electronic mass to the ionic mass. Strong-coupling corrections due to quasiparticle-quasiparticle scattering appear at the next order in (T_c/T_F). These corrections are known to be important in superfluid ^{3}He where $T_c/T_F \sim 10^{-2}$. Even though T_c is small in the heavy-fermion systems, the effective degeneracy temperature is also small, and $T_c/T_F \sim 10^{-2}$ or larger. Strong-coupling corrections due to quasiparticle-quasiparticle scattering may thus be important in the heavy-fermion superconductors; evidently they are unimportant in an ordinary superconductor where $T_c/T_F \sim 10^{-4}$ or smaller.

In a conventional BCS superconductor, the weak attractive interaction between electrons is mediated by phonons. The ratio T_D/T_F, where T_D is the Debye temperature, is small, allowing one to treat accurately even a strong electron-phonon interaction in second order. In the heavy-fermion systems, this ratio is evidently of order unity, and the validity of this theory is unclear.

The narrow bandwidth of the f electrons suggests that the repulsive interaction between quasiparticles due to the Coulomb interaction should be important in these materials. In liquid ^{3}He, strong short-ranged repulsive interactions between ^{3}He quasiparticles discourage Cooper pairing in a relative s-wave state, and the quasiparticles form a Cooper pair in a relative p-wave state. Analogies with liquid ^{3}He gave rise to the initial speculation that the quasiparticles forming the condensate wave function in the heavy-fermion superconductors are in a relative angular momentum state with $l > 0$. The strong intrasite repulsion between electrons on f sites also gives rise to spin fluctuations in the normal state. Analogy to liquid ^{3}He suggests that spin fluctuations, rather than phonons, may provide the attractive interaction between quasiparticles. The mechanism for pairing in the heavy-fermion systems and the microscopic description of the superconducting state are topics of considerable controversy and lie outside the scope of this work. We refer the reader to Lee *et al.* (1986) and Fulde *et al.* (1988) for reviews.

The determination of whether heavy-fermion superconductors are conventional or unconventional rests on the interpretation of experiments that probe the symmetry of the order parameter. The apparent absence of small parameters has prompted an approach that relies primarily on symmetry and on the most fundamental assumptions. Thus a considerable effort has been devoted to exploring the predictions of Ginzburg-Landau (GL) theories of unconventional superconductors. The connection between GL theory and microscopic theory has been studied carefully for superfluid ^{3}He, the archetypal unconventional "superconductor." Superfluid ^{3}He shows two distinct superfluid phases in the temperature-pressure phase diagram. At low pressure the B phase is stable, consistent with weak-coupling BCS theory. As a result of strong-coupling corrections, the A phase becomes stable at high pressure. The form of the Ginzburg-Landau free energy is dictated by symmetry; the value of the parameters that appear in the free-energy functional may be calculated from microscopic theory or deduced from experiments.

The normal-to-superconducting transformation can be viewed as a second-order phase transition in which quasiparticles form a condensate of Cooper pairs. A natural order parameter describing the superconducting state is the condensate wave function,

$$\langle \psi_\alpha(\mathbf{R}+\mathbf{r})\psi_\beta(\mathbf{R}-\mathbf{r})\rangle, \tag{27}$$

where $\mathbf{R}$ and $\mathbf{r}$ are the center of mass and relative coordinates of the quasiparticles in the Cooper pair, and $\psi_\alpha(\mathbf{r})$ is a field operator that destroys a particle of spin α at $\mathbf{r}$. It is a general property of a second-order phase transition that a symmetry of the normal state is broken in the ordered state. In the superconducting state, the gauge symmetry of the normal state is broken by the appearance of the condensate wave function. In an unconventional superconductor, not only is gauge symmetry broken, but a symmetry or symmetries of the crystalline lattice may also be broken because the condensate wave function has a lower symmetry than the crystal lattice. For example, because ^{3}He quasiparticles are paired in a spin-triplet orbital p-wave state,

parity is broken, and ^{3}He is an unconventional superfluid.

In the heavy-fermion systems, strong spin-orbit coupling breaks full rotational symmetry in spin space, but the crystal structures have a center of inversion symmetry, so that the notions of "singlet" and "triplet" states should be replaced by "even-parity" and "odd-parity" states. The condensate wave function may still be written as above if α and β are interpreted as pseudospin labels.

The general theory of second-order phase transitions allows the possible unconventional superconducting states to be classified according to the symmetry of the condensate wave function, without making assumptions about the nature of the pairing interaction or the extent of strong-coupling corrections to the superconducting state. Here, we give a heuristic explanation of the symmetry classification of the superconducting order parameter, based on weak-coupling BCS theory. A gap matrix related to the condensate wave function is defined by the expression

$$\Delta_{\mathbf{k},\alpha\beta} = \sum_{\mathbf{k}'} V^{\alpha\beta;\gamma\delta}(\mathbf{k},\mathbf{k}')\langle\psi_\gamma(\mathbf{k})\psi_\delta(\mathbf{k}')\rangle, \qquad (28)$$

where $\langle\psi_\gamma(\mathbf{k})\psi_\delta(\mathbf{k}')\rangle$ is the Fourier transform of the condensate wave function and $V^{\alpha\beta;\gamma\delta}(\mathbf{k},\mathbf{k}')$ is the generally spin-dependent pairing interaction. The gap equation separates by symmetry representation, and there is a transition temperature T_c^i for the ith representation. Generally only one representation will occur at the physical T_c, although more than one may be present because of the occurrence of "accidental degeneracies." For order parameters of lower symmetry, the nonlinear gap equation can couple order parameters from different representations so that other representations may be induced below T_c. This has been discussed for ^{3}He by Leggett (1975) and reviewed in more detail along with the symmetry classification by Sigrist and Ueda (1991). A group-theoretical analysis for strong spin-orbit coupling is given by Volovik and Gor'kov (1985) and Blount (1985), and the weak spin-orbit coupling case is discussed by Ozaki *et al.* (1985). A GL theory of the superconducting state can be constructed once the symmetry of the order parameter is known.

As we have noted, at sufficiently low temperatures it is generally accepted that the heavy-fermion systems behave like Landau Fermi liquids. Many authors have used this as justification to proceed with a BCS description of the superconducting state (Sigrist and Ueda, 1991; Lee *et al.*, 1986). The connection between the condensate wave function and the quasiparticle dispersion relation is dependent on the theoretical description of the superconducting state. In BCS theory for a singlet superconductor, the quasiparticle energy is related to the gap function $\Delta(\mathbf{k})$ through

$$E_\mathbf{k} = \sqrt{e_\mathbf{k}^2 + |\Delta(\mathbf{k})|^2}. \qquad (29)$$

The gap function of an unconventional superconductor may vanish for points or lines on the Fermi surface, which can be determined from the symmetry classification. Such an analysis shows (Blount, 1985) that for strong spin-orbit coupling, odd-parity states have no nodal lines. The thermodynamic and transport data described above suggest that the gap function of the heavy-fermion superconductors vanishes on points or lines, giving rise to power-law (rather than thermally activated) behavior at low temperatures. Detailed calculations of these properties for various unconventional superconducting states show a strong dependence of the "power law" on impurity scattering (see Sigrist and Ueda, 1991), making an unambiguous identification of the superconducting state impossible.

Other experiments have been proposed to probe the symmetry of the order parameter. A GL-theory analysis of upper critical fields by Gor'kov and by Burlachkov (see Gor'kov, 1987) showed that the reduced symmetry of an unconventional order parameter can lead to unusual upper-critical-field anisotropies. For example, the upper critical field in the basal plane of a tetragonal crystal might appear in contour like a four-leaf clover. Similar anisotropies would be apparent in H_{c1}.

The order parameter describing an unconventional superconductor often has more degrees of freedom than its conventional counterpart, and there often exist degenerate superconducting states. Some tests for unconventional superconductivity rest on the consequences of lifting a degeneracy between different superconducting states. Joynt and Rice (1985) showed that the condensation to an unconventional superconducting phase described by an order parameter with lower symmetry than the crystal lattice would be

accompanied by a lattice distortion. This effect can be "inverted" by applying a uniaxial stress that induces a splitting of the superconducting transition. The transition to the unconventional superconducting state may break time-reversal symmetry, for example, resulting in a weak magnetic moment, which may explain the small magnetic moment observed below the lower-temperature transition in $U_{1-x}Th_xBe_{13}$. Tokuyasu *et al.* (1990) showed that broken time-reversal symmetry can also result in an unusual anisotropy of H_{c1}. Reversing the direction of the field applied along a high-symmetry direction in an unconventional superconductor with broken time-reversal symmetry creates a vortex state that is inequivalent to that for the original field direction, resulting in a different value for H_{c1}. For this effect to occur, it is crucial that one time-reversal symmetry-breaking state cannot be continuously deformed into the other as is the case in a crystal of uniaxial symmetry. Other tests are reviewed in Gor'kov (1987) and Sigrist and Ueda (1991).

As a superconductor is cooled through the phase transition, different states may nucleate in different areas of the sample and domain walls form. Generally, the presence of domains obscures the simple tests described above. For example, the anisotropy of the upper critical field can be obscured by randomly oriented superconducting domains.

Perhaps the most compelling evidence for unconventional superconductivity is the intriguing H-T phase diagram of UPt_3 (see Fig. 7) and the thorium-substitution phase diagram of $U_{1-x}Th_xBe_{13}$ (see Fig. 6). The explanation of these phase diagrams is controversial; however, we will discuss the most developed ideas in the area to illustrate some additional tests for unconventional superconductivity.

A promising model for UPt_3 assumes that the order parameter η has two complex components as allowed by the hexagonal symmetry of the crystal together with the assumption of strong spin-orbit coupling (Tokuyasu *et al.*, 1990). Numerical solutions of the Ginzburg-Landau equations (Tokuyasu *et al.*, 1990; Tokuyasu and Sauls, 1990) for vortices along the c axis in the time-reversal symmetry-breaking homogeneous phases $\eta^{\pm} \sim (1, \pm i)$ suggest an explanation for the line separating phases I and II in Fig. 7. For a range of parameters entering the GL free energy, Tokuyasu showed that the low-field solution of the GL equations is a triangular lattice of vortices each axially symmetric, threaded by two quanta of magnetic flux, and having a finite superfluid density in the core. At a higher field ($\sim 0.3H_{c2}$), this lattice becomes unstable and abruptly transforms into a distorted lattice of single-flux-quantum vortices. A phase line like that shown separating phases II and III in Fig. 7 occurs as a result of the coupling of the order parameter to a symmetry-breaking field that lifts the twofold degeneracy of the pairing interaction (see for example, Hess *et al.*, 1989; Garg, 1992). In zero field, the phase transition is split into two: a transition from the normal state to a superconducting state described by a single complex component, e.g., $\eta \sim (1,0)$, and a lower-temperature transition from the superconducting phase to another superconducting phase that approaches η^+ or η^- with decreasing temperature. A natural candidate for the symmetry-breaking field is the weak antiferromagnetic order in the basal plane that has recently been correlated with the splitting of T_c (Hayden *et al.*, 1992). The additional phase lines in the mixed state may not be true phase lines but may rather mark regions of rapid crossover (Garg, 1992).

Attempts to understand the x-T phase diagram of $U_{1-x}Th_xBe_{13}$ assume that superconducting states belonging to two different representations are involved. A simple model with coupled s- and d-wave order parameters was considered by Kumar and Wölfle (1987). In their picture, pure UBe_{13} is a d-wave superconductor in the vicinity of the phase transition. As the temperature is lowered, s-wave character mixes in smoothly without introducing a second phase transition. Since a gap of lower symmetry is generally more sensitive to impurities, the effect of doping is to reduce the d-wave transition temperature dramatically so that above the critical concentration, the high-temperature transition is to an s-wave state. At lower temperatures a transition to a state described by a d-wave order parameter occurs. Sigrist and Rice (1989) took into account the cubic symmetry of the crystal and supposed that the pairing interaction leads to order parameters for two or more representations having nearly the same transition temperature. They explored the simple possibilities for various representations and concluded that the most promising phase diagram has an order parameter belonging to the Γ_1 (or Γ_5)

(one- or three-dimensional, respectively) representation for $x < x_c$, while for $x > x_c$ and $T > T_{c2}$ (see Fig. 6) the Γ_5 (or Γ_1) representation appears. For $T < T_{c2}$ the order parameter breaks time-reversal symmetry and belongs to a mixture of the two representations.

3. SUMMARY

The heavy-fermion materials are characterized by f electrons that exhibit localized behavior at high temperatures and itinerant behavior at low temperatures. The transformation from one regime to another suggests the existence of a characteristic energy scale. The entropy associated with the high-temperature magnetic moments is retained down to very low temperatures and appears in a specific heat that goes linearly with temperature. The slope of the specific heat at low temperature is anomalously large and suggests a narrow band of electrons characterized by an enormous effective mass. This state appears to be well described by Fermi-liquid theory, but it is unclear how such a state is formed from a lattice of weakly interacting magnetic moments. Taken as a dense lattice of local moments, the single-impurity Anderson model seems to be useful in discussing the high-temperature properties of these materials. Approximate methods applied to a model containing a dense lattice of Anderson impurities appear to yield the essential physics required to understand the heavy-fermion phenomena.

Many of these materials display unusual ordered ground states at low temperatures. Particularly interesting is the superconducting state that can apparently coexist with weak antiferromagnetic order. The unusual nature of the superconductivity suggests an order parameter of lower symmetry than that of the crystal lattice and a pairing interaction of electronic origin. The magnetic state is characterized by small magnetic moments associated with the f-atom sites and a simple magnetic structure. Although the magnitude of the magnetic moments is intimately connected with the removal of residual entropy, it is utterly unclear why so little entropy is associated with these transitions.

ACKNOWLEDGMENTS

We would like to thank J. D. Thompson for helpful conversations. We are also indebted to A. Y. Liu for useful suggestions and to J. W. Serene for a critical reading of the manuscript. Work at Los Alamos performed under the auspices of the U.S. Department of Energy.

GLOSSARY

BCS Theory of Superconductivity: Microscopic weak-coupling mean-field theory of superconductivity developed by Bardeen, Cooper, and Schrieffer in which electrons of opposite spin and momenta are paired by a weak attractive interaction.

Effective Mass: A parameter introduced as a renormalization of the electronic mass that takes into account the effect of the crystalline environment on the electronic energy spectrum. It includes the effect of interactions with other electrons and with the periodic potential of the atomic lattice.

Fermi Liquid: A macroscopic system of strongly interacting Fermi particles that can be described for energies and temperatures small compared to the degeneracy temperature as a gas of Fermi excitations (quasiparticles) with an effective mass different from that of a free constituent particle.

Hartree-Fock Approximation: An approximate treatment of the interactions between particles, obtained by replacing the effect of the other particles with a self-consistently chosen potential.

Hybridization: A quantum-mechanical admixture of atomic single-particle states, generally of differing symmetry.

Kondo Problem: The problem of describing a local magnetic impurity in a simple metallic environment.

Local-Density Approximation: An approximation made within the framework of density-functional theory for calculating electronic structure, in which the term representing the effects of electronic interactions is approximated by a quantity that depends only on the local electron density.

Mixed-Valence Materials: Materials containing elements of the lanthanide series, notably cerium, samarium, europium, thulium,

and ytterbium, which show properties characteristic of a strong admixture of two or more f configurations in the ground state.

Unconventional Superconductivity: A superconducting state with an order parameter that breaks not only gauge symmetry (because the pair wave function is complex), but also some other symmetry of the crystal point group. In a conventional superconductor, only gauge symmetry is broken.

List of Works Cited

Adenwalla, S., Lin, S. W., Ran, Q. Z., Zhao, Z., Ketterson, J. B., Sauls, J. A., Taillefer, L., Hinks, D., Levy, M., Sarma, B. K. (1990), *Phys. Rev. Lett.* **65**, 2298–2301.

Aeppli, G., Bucher, E., Goldman, A. I., Shirane, G., Broholm, C., Kjems, J. K. (1988), *J. Magn. Magn. Mater.* **76&77**, 385–390.

Allen, J. W. (1988), *J. Magn. Magn. Mater.* **76&77**, 324–330.

Allen, J. W., Oh, S.-J., Cox, L. E., Ellis, W. P., Wire, M. S., Fisk, Z., Smith, J. L., Pate, B. B., Lindau, I., Arko, A. J. (1985), *Phys. Rev. Lett.* **54**, 2635–2638.

Allen, J. W., Oh, S.-J., Gunnarson, O., Schönhammer, K., Maple, M. B., Torikachvili, M. S., Lindau, I. (1986) *Adv. Phys.* **35**, 275–316.

Amato, A., Feyerherm, R., Gygax, F. N., Schenck, A., Weber, M., Caspary, R., Hellman, P., Schank, C., Geibel, C., Steiglich, F., MacLaughlin, D. E., Knetsch, E. A., Heffner, R. H. (1992), *Europhys. Lett.* **19**, 127–133.

Anderson, P. W. (1961) *Phys. Rev.* **124**, 41–53.

Andres, K., Graebner, J. E., Ott, H. R., (1975), *Phys. Rev. Lett.* **35**, 1779–1782.

Arko, A. J., Koelling, D. D., Reihl, B. (1983), *Phys. Rev. B* **27**, 3955–3961.

Arko, A. J., Koelling, D. D., Dunlap, B. D., Mitchell, A. W. (1988), *J. Appl. Phys.* **63**, 3680–3682.

Baym, G., Pethick, C. J. (1978), in: K. H. Bennemann, J. B. Ketterson (Eds.), *The Physics of Liquid and Solid Helium*, Vol. 2, New York: Wiley, p. 1.

Beyermann, W. P., Hundley, M. F., Canfield, P. C., Thompson, J. D., Fisk, Z., Smith, J. L., Selsane, M., Godart, C., Latroche, M. (1991), *Phys. Rev. Lett.* **66**, 3289–3692.

Bickers, N. E., (1987), *Rev. Mod. Phys.* **59**, 845–939.

Blount, E. I., (1985), *Phys. Rev. B* **32**, 2935–2944.

Brodale, G. E., Fisher, R. A., Phillips, N. E., Stewart, G. R., Giorgi, A. L. (1986), *Phys. Rev. Lett.* **57**, 234–237.

Bruls, G., Weber, D., Wolf, B., Thalmeier, P., Lüthi, B., de Visser, A., Menovsky, A. (1990), *Phys. Rev. Lett.* **65**, 2294–2297.

Carneiro, G. M., Pethick, C. J. (1975), *Phys. Rev. B* **11**, 1106–1124.

Chapman, S., Hunt, M., Meeson, P., Reinders, P. H. P., Springford, M., Norman, M. (1990), *J. Phys. Condens. Matter* **2**, 8123–8136.

Czycholl, G. (1986), *Phys. Rep.* **143**, 277–346.

Fisher, R. A., Kim, S., Woodfield, B. W., Phillips, N. E., Taillefer, L., Hasselbach, K., Floquet, J., Giorgi, A. L., Smith, J. L. (1989), *Phys. Rev. Lett.* **62**, 1411–1414.

Fisk, Z., Smith, J. L., Ott, H. R., Batlogg, B. (1985), *J. Mag. Magn. Mater.* **52**, 79–84.

Fisk, Z., Hess, D. W., Pethick, C. J., Pines, D., Smith, J. L., Thompson, J. D., Willis, J. O. (1988), *Science* **239**, 33–42.

Freeman, A. J., Min, B. I., Norman, M. R. (1987), in: K. A. Gschneidner, Jr., L. Eyring, S. Hufner (Eds.), *The Handbook on the Physics and Chemistry of the Rare-Earths*, Vol. 10, Amsterdam: North-Holland.

Fulde, P., Keller, J., Zwicknagl, G. (1988), in: H. Ehrenreich and D. Turnbull (Eds.), *Solid State Physics* Vol. 41, New York; Academic.

Garg, A. (1992), *Phys. Rev. Lett.* **69**, 676–679.

Geibel, C., Schank, C., Thies, S., Kitazawa, H., Bredl, C. D., Böhm, A., Rau, M., Grauel, A., Caspary, R., Helfrich, R., Ahlheim, U., Weber, G., Steglich, F. (1991) *Z. Phys. B.* **84**, 1-2.

Gor'kov, L. P. (1987), *Sov. Sci. Rev. A Phys.* **9**, 1-116.

Gutzwiller, M. C. (1965), *Phys. Rev.* **137**, A1726–A1735.

Haldane, F. D. M. (1978), *Phys. Rev. Lett.* **40**, 416–419.

Hayden, S. N., Taillefer, L., Vettier, C., Floquet, J. (1992) *Phys. Rev. B* **46**, 8675-8678.

Hess, D. W., Tokuyasu, T. A., Sauls, J. A. (1989), *J. Phys. Condens. Matter* **1**, 8135–8145.

Horvatić, B., Zlatić, V. (1985), *Solid State Commun.* **54**, 957–960.

Hundley, M. F., Canfield, P. C., Thompson, J. D., Fisk, Z. (1990), *Phys. Rev. B* **42**, 6842–6845.

Jones, B. A., Varma, C. M., Wilkins, J. W. (1988), *Phys. Rev. Lett.* **61**, 125–128.

Joynt, R., Rice, T. M. (1985), *Phys. Rev. B* **32**, 6074–6076.

Kjems, J. K., Broholm, C. (1988), *J. Magn. Magn. Mater.* **76&77**, 371–375.

Kohn, W., Sham, L. J. (1965), *Phys. Rev.* **140**, A1133–A1138.

Krishnamurthy, H. R., Wilkins, J. W., Wilson, K. G. (1980), *Phys. Rev. B* **21**, 1003–1044.

Kumar, P., Wölfle, P. (1987), *Phys. Rev. Lett.* **59**, 1954–1957.

Lee, P. A., Rice, T. M., Serene, J. W., Sham, L. J., Wilkins, J. W. (1986), *Comments Condens. Mater. Phys.* **12**, 99.

Leggett, A. J. (1975), *Rev. Mod. Phys.* 47, 331–414.

Liu, S. H., Ho, K.-M. (1982), *Phys. Rev. B* **26**, 7052–7055.

Lüthi, B. (1985), *J. Magn. Magn. Mater.* **52**, 70–78.

MacLaughlin, D. E. (1985), *J. Magn. Magn. Mater.* **47&48**, 121-126.

Newns, D. M., Read, N. (1987), *Adv. Phys.* **36**, 799–849.

Nozières, P. (1974), *J. Low Temp. Phys.* **17**, 31–42.

Nozières, P. (1985), *Ann. Phys. (Paris)* **10**, 19–35.

Ott, H. R., Fisk, Z. (1987) in: A. J. Freeman, G. H. Lander (Eds.), *Handbook on the Physics and Chemistry of the Actinides*, Vol. 5, Amsterdam: North-Holland.

Ott, H. R., Rudigier, H., Fisk, Z., Smith, J. L. (1983), *Phys. Rev. Lett.* **50**, 1595–1598.

Ozaki, M., Machida, K., Ohmi, T. (1985), *Prog. Theor. Phys.* **74**, 221–235.

Palstra, T. T. M., Menovsky, A. A., van den Berg, J., Dirkmaat, A. J., Kes, P. H., Nieuwenhuys, G. J., Mydosh, J. A. (1985) *Phys. Rev. Lett.* **55**, 2727-2730.

Parks, R. D. (1969), *Superconductivity*, 2 volumes, New York: Marcel Dekker.

Pethick, C. J., Pines, D. (1987) in: P. Siemens, R. Smith (Eds.), *Proceedings of the International Conference on Recent Progress in Many-Body Theoretical Physics*, Vol. 4, Berlin: Springer Verlag.

Rainer, D. (1988), *Phys. Scr.* **T23**, 106–112.

Rice, T. M., Ueda, K. (1985), *Phys. Rev. Lett.* **55**, 995–998.

Rossat-Mignod, J., Regnault, L. P., Jacoud, J. L., Vettier, C., Lejay, P., Floquet, J., Walker, E., Jaccard, D., Amato, A. (1988), *J. Magn. Magn. Mater.* **76&77**, 376–384.

Rossel, C., Yang, K. N., Maple, M. B., Fisk, Z., Zirngieble, E., Thompson, J. D. (1987), *Phys. Rev. B* **35**, 1914–1918.

Schlottmann, P. (1989), *Phys. Rep.* **181**, 1–119.

Schoenes, J., Franse, J. J. M. (1986), *Phys. Rev. B* **33**, 5138–5140.

Schrieffer, J. R. (1964), *Theory of Superconductivity*, Redwood City, CA: Addison-Wesley.

Schrieffer, J. R., Wolff, P. A. (1966), *Phys. Rev.* **149**, 491–492.

Schweitzer, H., Czycholl, B. (1990), *Solid State Commun.* **74**, 735–742.

Sigrist, M., Rice, T. M., (1989), *Phys. Rev. B* **39**, 2200–2216.

Sigrist, M., Ueda, K. (1991), *Rev. Mod. Phys.* **63**, 239–311.

Slichter, C. P. (1978), *Principles of Magnetic Resonance*, Berlin: Springer, p. 156.

Smith, J. L. (1992), *Philos Mag. B* **65**, 1367–1371.

Steglich, F., Aarts, J., Bredl, C. D., Lieke, W., Meschede, D., Franz, W., Schäfer, J. (1979), *Phys. Rev. Lett.* **43**, 1892–1896.

Stewart, G. R., (1984), *Rev. Mod. Phys.* **56**, 755–787.

Taillefer, L., Newbury, R., Lonzarich, G. G., Fisk, Z., Smith, J. L. (1987), *J. Magn. Magn. Mater.* **63&64**, 372–376.

Takabatake, T., Teshima, F., Fujii, H., Nishigori, S., Suzuki, T., Fujita, T., Yamaguchi, Y., Sakuri, J. (1990), *Phys. Rev. B* **41**, 9607–9610.

Tien, C., MacLaughlin, D. E., Lan, M. D., Clark, W. G., Fisk, Z., Smith, J. L., Ott, H. R. (1985), *Physica B 135*, 14–21.

Tokuyasu, T. A., Sauls, J. A. (1990), *Physica B* **165&166**, 347–348.

Tokuyasu, T. A., Hess, D. W., Sauls, J. A. (1990), *Phys. Rev. B* **41**, 8891–8903.

Tsvelick, A. M, Wiegman, P. B. (1983), *Adv. Phys.* **32**, 453–713.

de Visser, A. (1986), Ph.D. thesis, University of Amsterdam, unpublished.

Volovik, G. E., Gor'kov, L. P. (1985) *Zh. Eksp. Teor. Fiz.* **88**, 1412–1428 [*Sov. Phys. JETP* **61**, 843–854 (1985)].

Wang, C. S., Norman, M. R., Albers, R. C., Boring, A. M., Pickett, W. E., Krakauer, H., Christensen, N. E. (1987), *Phys. Rev. B* **35**, 7260–7263.

Weber, D., Yoshizawa, M. Kouroudis, I., Lüthi, B., Walker, E. (1987) *Europhys. Lett.* **3**, 827-831.

Yoshizawa, M., Lüthi, B., Goto, T., Suzuki, T., Renker, B., de Visser, A., Frings, P., Franse, J. J. M. (1985), *J. Magn. Magn. Mater.* **52**, 413-417.

Further Reading

Fisk, Z., Ott, H. R., Rice, T. M., Smith, J. L. (1986), *Nature* **320**, 124-129. A valuable experimental review with emphasis on the superconductors.

Fisk, Z., Hess, D. W., Pethick, C. J., Pines, D., Smith, J. L., Thompson, J. D., Willis, J. O. (1988), *Science* **239**, 33-42. A combined theory and experiment overview with some emphasis on the Fermi-liquid character of the low-temperature heavy-fermion state.

Fulde, P., Keller, J., Zwicknagel, G. (1988), in: H. Ehrenreich, D. Turnbull (Eds.), *Solid State Physics*, Vol. 41, New York: Academic. A summary of efforts to formulate a theory of heavy-fermion systems, more recent than the following.

Gor'kov, L. P. (1987), *Sov. Sci. Rev. A Phys.* **9**, 1-116. A review from a theoretical perspective emphasizing unconventional superconductivity.

Grewe, N., Steglich, F. (1990), in: K. A. Gschneidner, L. Eyring (Eds.), *Handbook on the Physics and Chemistry of the Rare Earths*, Vol. 13, New York: Elsevier. Another summary like that of Fulde *et al.*

Lee, P. A., Rice, T. M., Serene, J. W., Sham, L. J., Wilkins, J. W. (1986), *Comments Condens.-Matter Phys.* **12**, 99-154. A critical review of efforts to formulate a theory of heavy-fermion systems.

Ott, H. R., Fisk, Z. (1987), in: A. J. Freeman, G. H. Lander (Eds.), *Handbook on the Physics and Chemistry of the Actinides*, Vol. 5, Amsterdam:

North-Holland. This and the following provide valuable experimental overviews and insights.

Ott, H. R. (1987), in: D. F. Brewer (Ed.), *Progress in Low Temperature Physics XI*, Amsterdam: North-Holland, pp. 215-289.

Sarma, B. K., Levy, S., Adenwalla, S., Ketterson, B. (1992), in: M. Levy (Ed.), *Physical Acoustics*, Vol. 20, Boston: Academic. A review of heavy-fermion superconductors with particular emphasis on sound experiments.

Sigrist, M., Ueda, K. (1991), Rev. Mod. Phys. **63**, 239-311. A review at some length of unconventional superconductivity.

Stewart, G. R. (1984), Rev. Mod. Phys. **56**, 755-787. A review of experiments up to that time.